DEVELOPMENT OF A HORIZONTAL ZONE REFINER FOR OPTIMIZATION STUDIES

by

Jordan Haas

B. Eng, University of Victoria May 2002.

Submitted in partial fulfillment of requirements for the degree

MASTERS OF APPLIED SCIENCE

in the department of Mechanical Engineering.

DEVELOPMENT OF A HORIZONTAL ZONE REFINER FOR OPTIMIZATION STUDIES

by

Jordan Haas

B. Eng, University of Victoria May 2002.

Supervisory Committee:

Dr. Sadik Dost	(Department of Mechanical Engineering)
Supervisor	
Dr. Andrew Rowe	(Department of Mechanical Engineering)
Department Member	
Dr. Alexandre Brolo	(Department of Chemistry)
Outside Member	

Supervisory Committee:

Dr. Sadik Dost	(Department of Mechanical Engineering)
Supervisor	
Dr. Andrew Rowe	(Department of Mechanical Engineering)
Department Member	
Dr. Alexandre Brolo	(Department of Chemistry)
Outside Member	

ABSTRACT

Many of the physical properties of semiconductor materials depend on the presence of imperfections. A significant source of lattice imperfections is the inclusion of foreign atoms, or impurities; since most semiconductor devices require accurate and repeatable results, highly pure materials are desired. In order to obtain high purity semiconductor metals, zone purification is commonly utilized as the final purification stage. Due to the demand for increasing purity in an extremely competitive industry, producers must increase process efficiency and reduce production costs.

The University of Victoria Crystal Growth Lab Group (CGL) is participating in a project aimed at increasing the efficiency of a commercial zone refining system. The project is composed of two parts: a numerical analysis intended to simulate the process, and an experimental study intended to verify the numerical model and conduct optimization experiments. A zone refiner was designed and developed in the lab for the experimental portion of the project. This thesis details the experimental portion of the project.

The CGL zone refiner will be used to study the effects of zone geometry and mixing on the efficiency of the process. In order to achieve the most efficient possible combination, the zone refiner was constructed with the capability to adjust all of the typical process variables such as zone speed, zone spacing, and number of zone passes, as well as to accommodate specific methods aimed at increasing mixing in the melt such as applying an electric current or a rotating magnetic field.

Once the CGL zone refiner system was complete, several experiments were carried out to prove and characterize the system. Samples were removed from the purified ingots and sent for glow discharge mass spectrometry (GDMS) analysis. The GDMS results indicated that the CGL zone refiner purified the ingot as desired and that there were no external sources of contamination from the process; in general, a reduction in concentration was seen for the impurities tested.

During both the initial thermal testing and the subsequent full process experiments, the zone refiner performed as expected and without difficulty. The entire process was qualified and determined to be stable and easily controlled. The experiments conducted to date have shown that the system is a capable zone refiner for all of the planned studies.

TABLE OF CONTENTS

LIST OF FIGURES

LIST OF TABLES

ACKNOWLEDGEMENTS

I would like to thank Dr. Sadik Dost for his supervision and guidance, and Mr. Brian Lent for his continual support; without either of whom, this project would not have been possible.

I would also like to thank 5NPlus Inc. and the National Sciences and Engineering Research Council, both for their financial assistance and for creating the opportunity to conduct this research.

INTRODUCTION

The industrial applications and production of semiconductors have developed dramatically since the initial research with devices in the early 1950's. Today, semiconductors are used in various applications such as solar cells, power devices, imaging detectors and more [1]. Semiconductor materials can be utilized in their pure single crystal form, but are also commonly doped or compounded with other materials to obtain the specific optical and electric properties desired for a device.

Many of the properties of crystals depend on the presence of imperfections [2]. A significant source of lattice imperfections is the inclusion of foreign atoms, or impurities; even trace levels of impurities are known to have significant harmful effects on the performance of imaging devices [3], [4]. Since most semiconductor devices require highly accurate and repeatable results, extremely pure materials are required in order to obtain predictable and consistent properties.

Semiconductor materials are most commonly extracted from primary ores; these are then purified through various chemical, electrolytic and pyrometallurgical methods [1], [5]. The electrochemical procedures are utilized for the gross initial purification steps; they can achieve around 3-4N purity (99.9 – 99.99%), yet relatively high levels of impurities remain. Zone refining is commonly used as the last step in the purification process; it is an important final procedure in the purification of materials. Currently, materials are being commercially produced with purities up to and exceeding 7N (99.99999%) using zone refining.

Although there are indications that work was carried out with the process as early as the 1930's [6], zone refining was first introduced to the public in 1952 by Pfann [7]. The creation and quick advancement of rectifiers and transistors created a demand for high purity germanium after WWII; this produced a need for more effective purification methods. During this period Pfann stumbled across the idea of zone purification [8] and has since published many papers as well as a definitive book on the subject [9]. Zone refining usually takes advantage of the difference in composition between the solid and liquid phases, but it can be used to purify any material which has a varied composition between two phases. The technique has been applied to metals and semiconductors as well as to organic and inorganic compounds [10].

There has been a great deal of work since Pfann's initial publications; numerous papers document research conducted on zone refining of specific materials and various experimental techniques. As well as experimental work, there have been a number of numerical studies on the zone refining process; for example there are simulations aimed at understanding the zone refining process such as those presented by Ho et al. [11]-[14]. Optimization studies have been carried out by Rodway and Hunt [15], Spim et al. [16] and Ho et al. [17], which looked to optimize the process based on certain criteria for specific applications. Also, some recent studies such as those presented by Roussopoulos and Rubini [18] use computer numerical modelling to understand the thermal effects. A summary of zone refining theory, as well as an introduction to some of the existing modelling and optimization methods is provided in the first portion of this thesis.

Unfortunately, in the commercial sector of materials production there are limited resources for research. There is continuous pressure on producers to market ever higher purity materials at competitive rates; as a result, the main objective of companies is to

reduce costs. In order to achieve sustainable commercial production in an extremely competitive industry, increased process efficiency and reduced production costs are required.

The University of Victoria Crystal Growth Lab Group (CGL) is currently participating in a joint Natural Sciences and Engineering Research Council of Canada Collaborative Research and Development (NSERC-CRD) study of the zone refining process and apparatus. The main objective of this project is the identification and demonstration of optimum process parameters and equipment configuration that will allow for the production of larger ingots, while minimizing process time and maintaining or improving the process efficiency and overall material yield. The project is composed of two parts: a numerical analysis intended to simulate the process, and an experimental study used to verify the numerical model and conduct optimization experiments. Ultimately both the numerical and experimental studies will be utilized to identify critical process parameters and recommend modifications to the current commercial apparatus to improve the efficiency and/or overall material yield.

For the experimental portion of the project, a small scale zone refiner has been designed and developed. This apparatus was built specifically for the experimentation planned for the study, i.e. to study the effects of zone geometry and mixing on the efficiency of the process. The second part of this thesis documents the experimental portion of the project; it details the design, development and initial testing of the UVic CGL zone refiner. The design considerations, capability and operation of the apparatus are explained, details of the characterization testing are specified, and the results presented.

1 ZONE PURIFICATION

Zone melting refers to the various methods of controlling the distribution of impurities, or solutes, in a crystalline solid [9]. During the zone melting process, a series of molten zones pass through a charge in one direction and impurities travel with or opposite to the zones, concentrating them in one end of the charge. Using the difference in composition between the freezing solid and liquid phases, zone melting permits the manipulation of impurities distributed in a material; for example it can be used for purification (zone refining), uniformly distributing a desired impurity (zone levelling) and single crystal growth among others. Zone refining can be used for purification of any material that can be safely melted and that exhibits a difference in impurity concentration between the liquid and solid phases [9].

The following chapter provides a summary of the relevant theory of zone refining, as well as an overview of the experimental techniques and an introduction to some of the numerical models previously developed.

1.1 THEORY

When a relatively large amount of molten metal with low concentrations of impurities, or solute, is allowed to cool, the composition at the freezing interface is generally different from the melt. The composition in the freezing solid can be richer or poorer in solute; this results in a boundary layer in front of the freezing interface that has decreased or increased solute concentration (See Figure 1.1b). From this, it can be said

that the freezing interface either attracts or rejects impurities. The solute-rich (or depleted) boundary layer results in an inequilibrium of concentration in the melt, and diffusion takes place. Segregation occurs as the impurities diffuse through the melt, and the molten zone traverses along the ingot; the distribution of these impurities depends on the distribution coefficient k.

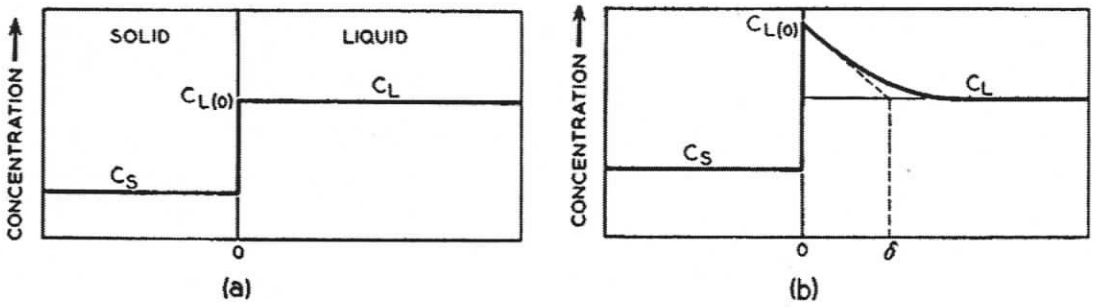

Figure 1.1: Solute concentration profiles for an advancing solid-liquid interface: a) equilibrium freezing, b) steady state [9].

1.1.1 THE DISTRIBUTION COEFFICIENT

The distribution coefficient can either be greater or less than unity, depending on whether the solute raises or lowers the melting point of the base material, or solvent [9] (See Figure 1.2). If the solute lowers the melting point of the solvent (k<1), its concentration in the freezing solid will be lower than in the liquid; therefore the impurity accumulates in the liquid. If the solute raises the melting point of the solvent (k>1), its concentration in the freezing solid will be higher than that in the liquid and the liquid will be depleted of the impurity.

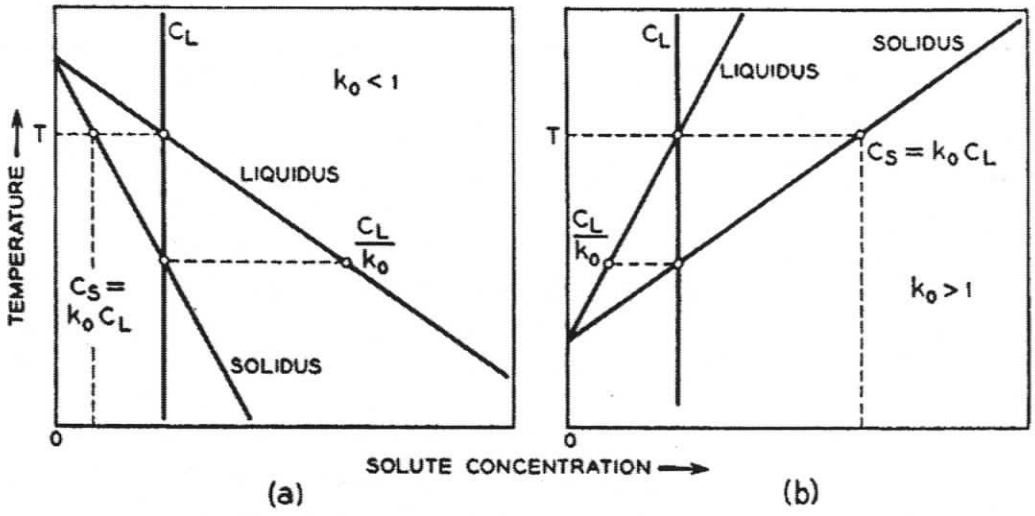

Figure 1.2: Portion of phase diagrams in which the freezing point of the solvent is a) lowered, b) raised by the solute or impurity [9].

1.1.2 NORMAL FREEZING

In order to understand the derivation of the distribution coefficient, we first examine normal and equilibrium freezing. Normal freezing occurs when a long charge of molten material freezes from one end (See Figure 1.3). The distribution of solute after freezing will not only depend on k, but also on the conditions of freezing such as solidification rate and degree of mixing in the melt [9]. At one extreme of these conditions is equilibrium freezing, in which the concentration and temperature gradients are negligibly small. This occurs if the freezing rate is slow enough to allow diffusion within the melt such that any concentration gradient in the boundary layer is eliminated [9] (See Figure 1.1a). During equilibrium freezing the concentration of solute in the solid remains constant and minimal purification can be achieved. The maximum purification factor that can be obtained is the equilibrium distribution coefficient k_0, and this is for only an infinitesimal amount of solid removed from the start of the ingot [9].

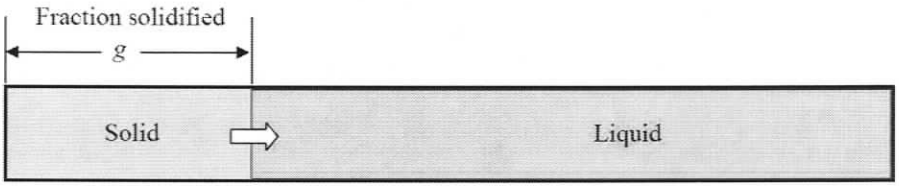

Figure 1.3: Schematic representation of normal freezing.

The equilibrium distribution coefficient can be taken from the phase diagram as shown in Figure 1.2 and is defined as the ratio of the solute concentration in the freezing solid to that in the main body of the liquid [9]:

$$k_0 = \frac{C_S}{C_L}$$

And the solute concentration after normal freezing is given by [9]:

$$C = kC_0(1-g)^{k-1}$$

where C_0 is the initial impurity concentration in the solid and C is the concentration at the location where a fraction g of the original liquid has frozen. Solute distribution curves after normal freezing for varied values of k are given in Figure 1.4.

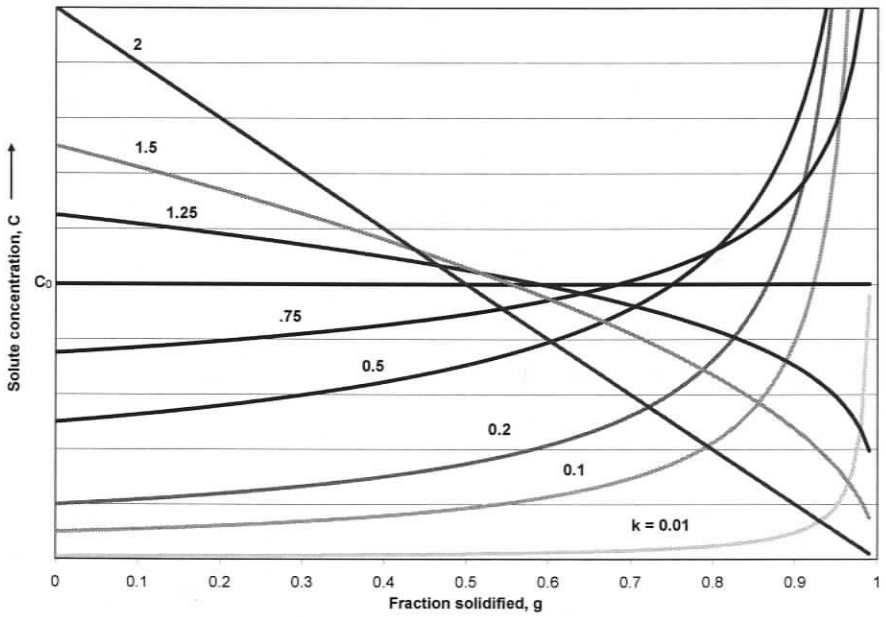

Figure 1.4: Distribution curves of normal freezing for various *k*.

1.1.3 THE EFFECTIVE DISTRIBUTION COEFFICIENT

The theoretically predicted equilibrium distribution coefficient is not usually observed under normal conditions because equilibrium freezing is rarely achieved [3]. This is due to the increased rate at which the advancing solid rejects the solute, creating an enriched layer ahead of the interface (or depleted for $k>1$). The term effective distribution coefficient k_{eff} (also simply referred to as the distribution coefficient, k) is used to describe the segregation of an impurity as observed in practice and is defined as the ratio of the solute concentration in the freezing solid to that in the enriched liquid boundary layer C_L^* ($k = C_S/C_L^*$). This can be calculated using the formula:

$$k = \frac{1}{1+(1/k_0 - 1)e^{-f\delta/D}}$$

where: f = growth rate (zone speed)

D = Diffusivity in the liquid

δ = boundary layer thickness

and $f\delta/D$ is known as the normalized growth velocity [9]. In addition to the equation above, recent studies have shown that the effective distribution coefficient of some impurities is also affected by the temperature of the melt [19]. Several different theories that attempt to quantify the effective distribution coefficient are summarized in [9].

Zone refining is usually divided into three cases for examination: after one pass, after successive passes, and after an indefinitely large number of passes. The ultimate distribution is achieved in this last case; it results in the maximum purification possible for a given ingot [9]. Equations for the first and last cases are easily derived, but for multiple zone passes, more advanced modelling is required.

1.1.4 SINGLE PASS DISTRIBUTION

Single pass zone refining refers to the case in which only a single molten zone is transported through the material (See Figure 1.5).

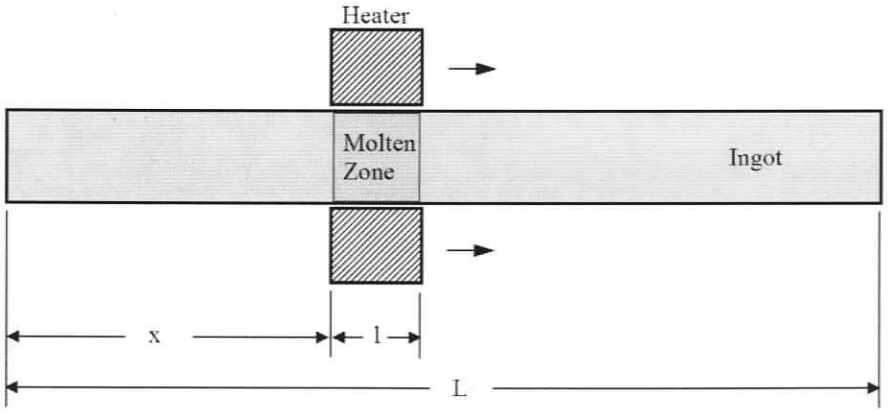

Figure 1.5: Single pass zone refining schematic.

After the molten zone has been passed through the ingot, the concentration profile typically contains three regions: an initial region, a level region, and a final region. The initial and final regions are the only ones in which solute concentration has changed; elsewhere, the concentration in the ingot remains the same as the initial concentration, C_0. This can be illustrated as follows: when the zone is first melted at the front of the ingot, its concentration is the same as that of the solid. As the zone starts to move and the first solid begins to freeze out, the concentration of solute in solid is lower than that of the melt (again, $k<1$ in this example). The concentration in the molten zone is increased at a decreasing rate by the rejected solute. As the zone progresses along the ingot, enrichment of the molten zone continues until the concentration reaches the value C_0/k. Once this concentration has been reached, the amount of solute entering and leaving the zone are equal, and the concentration of the freezing solid remains C_0 until the zone reaches the end of the ingot. Once at the end of the ingot, the solute-rich molten zone freezes out (normal freezing), resulting in higher concentrations.

An approximate concentration curve is shown in Figure 1.6 for a charge of initial concentration C_0 and $k<1$. The concentration after zone melting in the final region is given by the equation for normal freezing; the concentration for the initial and level regions can be described by the equation [9]:

$$\frac{C}{C_0} = 1 - (1-k)e^{-kx/l}$$

where l is the length of the molten zone and x is the distance from the point at which the first solid froze.

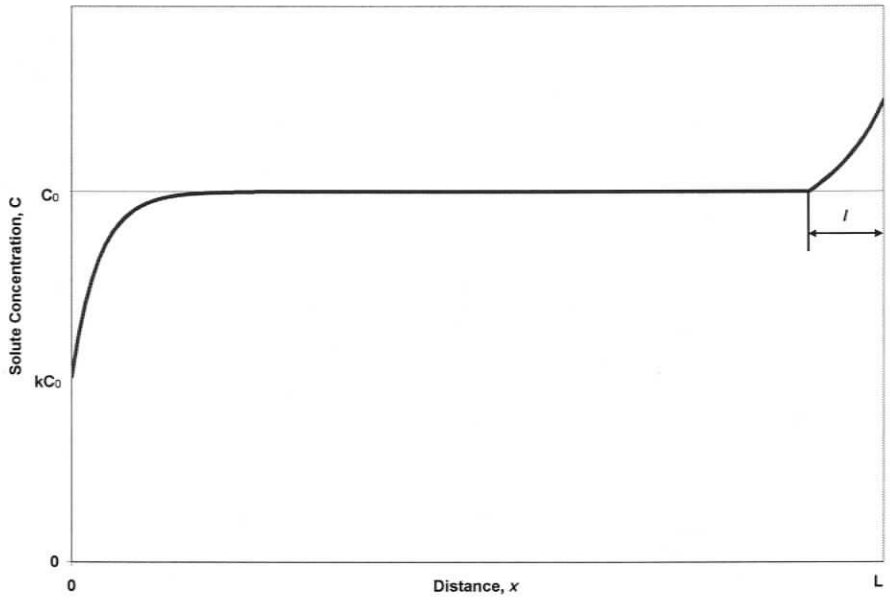

Figure 1.6: Typical single pass zone melting distribution [9].

1.1.5 MULTI-PASS DISTRIBUTION

The advantages of zone refining are only seen when multiple passes are used; single pass zone refining results in less purification than simple normal freezing [9]. By using a series of closely spaced heaters, any desired number of molten zones can be traversed through the ingot in a single operation, allowing for increased purification (See Figure 1.7). As shown in Figure 1.8a, the ingot initially has a semi-uniform distribution of impurities (O, o). As each successive molten zone passes through the ingot, impurities are segregated according to their respective distribution coefficient (Figure 1.8b, c). Once an appropriate number of molten zones have been passed, the ingot can be divided into three regions (Figure 1.8d). The initial region will contain higher concentrations of solute that raise the melting temperature of the material ($k>1$); the end region will contain higher concentrations of solute that lower the melting temperature of the material ($k<1$); and the middle region will be depleted of all solute with $k\neq1$.

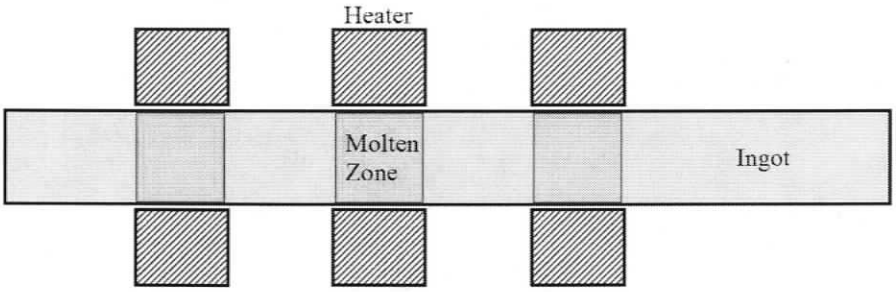

Figure 1.7: Multi-pass zone refining schematic.

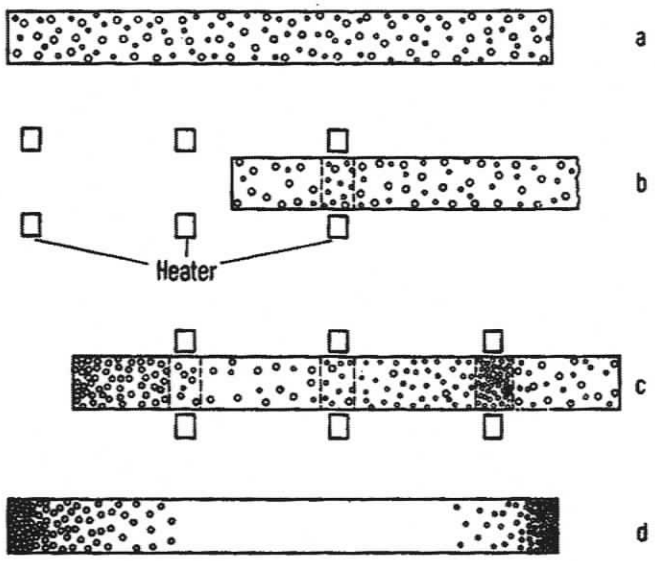

Figure 1.8: Segregation of impurities using multi-pass zone refining [20].

The distribution of solute after multi-zone refining is much more difficult to calculate than that of the normal or single zone distributions, and has been described briefly by Pfann [9]: consider a second pass over a single pass distribution as shown in Figure 1.6. As the zone passes through the initial region, additional solute is accumulated in the molten zone leaving behind a concentration profile with a longer and lower initial region. At the end of the ingot, the pile-up of solvent is reflected back one zone length during the second pass, and back one more, with decreasing intensity for each succeeding

pass. Additional passes lower the initial region, raise the end region, and decrease the length of the level region. Ultimately all three regions blend into a relatively smooth curve as shown in Figure 1.9.

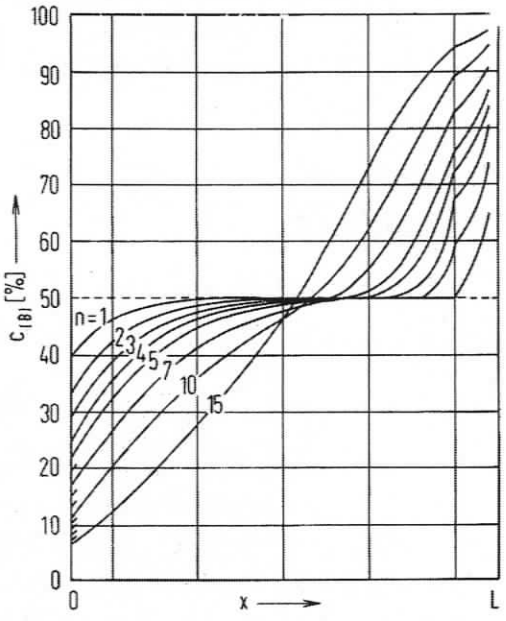

Figure 1.9: Approximate concentration curves after multiple passes [20].

1.1.6 ULTIMATE DISTRIBUTION

After numerous zone passes, the concentration distribution reaches a steady-state, or ultimate distribution. At this point, the amount of solute solidifying out at the freezing interface is equal to that which is added at the melting interface. An approximation to the ultimate distribution is given by the equation [9]:

$$C(x) = Ae^{Bx}$$

where the constants A and B can be obtained from:

$$k = \frac{Bl}{e^{Bl} - 1} \qquad A = \frac{C_0 BL}{e^{BL} - 1}$$

where C_0 is the initial impurity concentration, l is the molten zone length and L is the length of the ingot. This equation is only an approximation as it does not account for the normal freezing of the last zone [9]. An example of ultimate distributions for varied k values is shown in Figure 1.10.

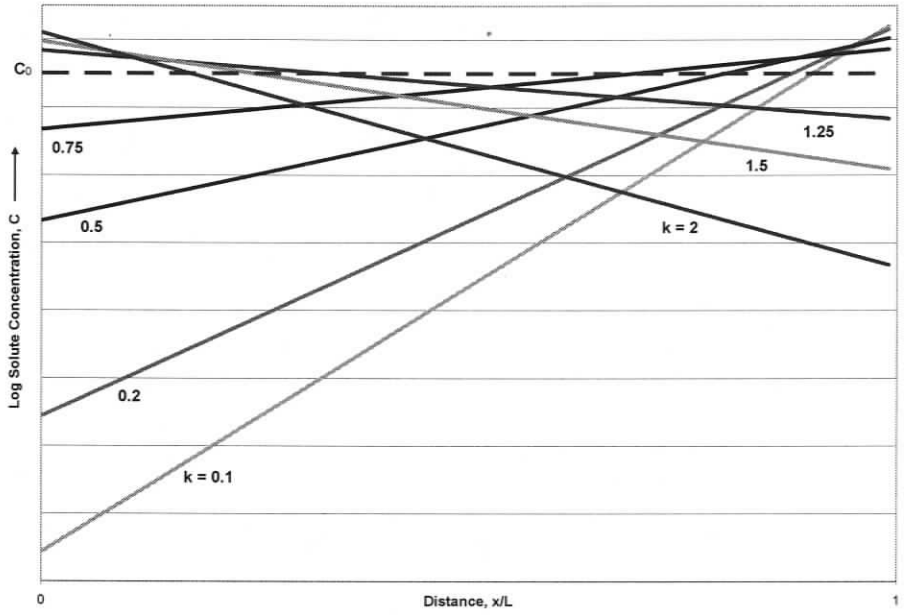

Figure 1.10: Ultimate distribution curves for various k; L=1, l=0.1.

1.1.7 MATERIAL TRANSPORT

Once successive molten zones have passed through a horizontal ingot, the ingot usually becomes tapered; this taper is due to matter transport associated with changes in density of the material upon melting [9]. The magnitude and direction of the matter transport corresponds to the magnitude and sign of the density change; contraction on melting causes forward transport (i.e. in the direction of travel), whereas expansion on melting causes reverse transport [9].

A schematic of forward transport is represented in Figure 1.11a. A molten zone (length l) is formed at the starting end of a level, horizontal ingot with height h_0. The height of the liquid will be αh_0, where α is the ratio of the solid to liquid densities. As the molten zone is advanced by dx, the volume of solid melted will be $h_0 dx$. The solid will freeze out at the height of the liquid, αh_0; the volume of solid frozen will be $\alpha h_0 dx$. Equations for calculating the height of the ingot are given by Pfann [9];

Zones 1 to n-1: $$\frac{h}{h_0} = 1 - (1-\alpha)e^{-\alpha x/l}$$

Final zone (normal freezing): $$\frac{h}{h_0'} = (1-g)^{\alpha-1}$$

where h_0' is the height of the liquid at the beginning of normal freezing and g is the fraction frozen.

Ultimate height distribution: $$\frac{h}{h_0} = A'e^{B'x} \qquad \alpha = \frac{B'l}{e^{B'l}-1} \qquad A' = \frac{B'L}{e^{B'L}-1}$$

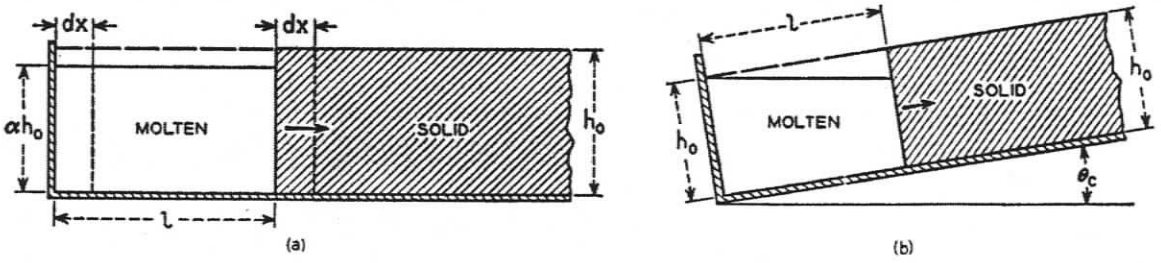

Figure 1.11: Matter transport upon melting and the critical tilting angle [9].

Matter transport during zone refining can be prevented by tilting the ingot at the proper angle as shown in Figure 1.11b. The critical tilt angle is given by the equation [9]:

$$\theta_C = \tan^{-1}\frac{2h_0(1-\alpha)}{l}$$

1.2 TECHNIQUES AND APPARATUS

1.2.1 ZONE REFINING METHODS

There are many diverse methods and apparatus for zone refining. For multi-zone refining alone, different charge shapes such as longitudinal, circular or spiral can be utilized. Many different heating, cooling, travel, and mixing methods are also available. If large quantities of material require purification, a non-batch process such as continuous zone refining is appropriate. Using this method a continuous flow of material is fed into the apparatus in which molten zones pass though; the purified product and waste materials are continuously removed from the respective "pure" and "impure" ends of the charge. One other important zone refining method is the float zone technique. This method utilizes surface tension to contain the melt, eliminating the need for containers and reducing the possibility of contamination.

A review of common equipment and processes is given below; information on the other various methods and apparatus can be found in [9] [20]-[22].

1.2.2 CONTAINMENT

Containers for zone refining must be non-reactive with the target material and contaminate the melt as little as possible. Proper cleaning of all apparatus – particularly the container - is essential to avoid contamination; an example cleaning procedure can be found in [23].

Common materials used for zone refining containers are glass, silica, graphite and oxides such as alumina, lime and magnesia [9], [20]. A review of the literature shows that the most common material used for zone refining tellurium is high purity quartz

[3],[4],[24],[25]. There are various longitudinal and cross-sectional shapes that can be used for zone refining; the most common is a straight cylinder with circular or semi-circular profile [9]. More examples of the shapes utilized are found in [9], [20].

Often, the containers used in zone refining must also provide an inert atmosphere for the process. It has been shown that zone refining under vacuum results in considerable purification due to impurity evaporation in addition to purification by segregation [26]. Alternatively, applied hydrogen gas flux through the system has been shown to enhance the purification of tellurium, especially for impurities with distribution coefficients close to one [27]; specifically, removal of selenium from tellurium is attained with high purity hydrogen gas flow. This is due to the reaction between the Se and H_2, which form hydrogen selenide; this gaseous compound is then carried away in the hydrogen stream. The use of ultra-pure hydrogen is required to avoid a black powder forming on the surface of the ingot due to impurities found in standard bottled hydrogen as reported by [4], [24].

1.2.3 HEATING

A few of the practical heating methods for semiconductor materials are resistance heating, thermostat heating and induction heating; the benefits of each are briefly discussed below. Additional heating methods can be found in [9], [20].

Resistance heating is the most common, simplest and most economical method. For moderately high melting materials, thermal insulation is usually installed around the heater to direct the heat flow and reduce the molten zone size. One of the limitations to this method is the air gap required between the heater and container; this gap contains thermal resistances that make it harder to control the molten zone. Additionally, the

heater must transmit through the container, resulting in the container being hotter than the charge; this increases the chance of contamination.

Thermostat heating utilizes heated (and cooled if necessary) plates or wires instead of current carrying wire. These heated plates can be placed closely side by side, which allows for variation of zone lengths [20]. A major limitation of this technique is the need for detached heating and cooling sources (to heat/cool plates as required). Along with the numerous heating and cooling paths to the plates, this creates a bulky and awkward apparatus.

Induction heating is produced as a result of electrical currents induced in the charge material by coils running alternating current placed around the charge. The amount of heating produced depends on the resistivity of the charge material and the frequency of the electrical coil. The benefits of this method are threefold: the heat is generated entirely within the charge reducing the possibility of contamination, eddy currents produced by induction provide some degree of stirring, and shorter zones can usually be achieved [20].

1.2.4 Cooling

Cooling is sometimes required for high melting materials or when finer control of the molten zone is desired. Cooling can also be beneficial in increasing the efficiency of zone refining; it is possible to use controlled cooling along with the heaters to manipulate the temperature gradients, which drive convective mixing as well as the molten zone size.

Simple methods of cooling are achieved from passive sources such as natural convection with the ambient air, or active forced air cooling. More complicated, but

higher performance cooling can be created using jackets, in which cooled water (or other fluid) pass through.

1.2.5 MIXING

Mixing of the molten zone is critical to the performance of zone refining. This is evident from the equation for the effective distribution coefficient given earlier: mixing reduces the thickness of the boundary layer at the freezing interface, which causes the effective distribution coefficient to approach the equilibrium distribution coefficient and results in better segregation.

Mixing of the molten zone occurs naturally as a result of differences in density due to temperature and/or concentration [9], but can also be produced deliberately in various ways as shown in Figure 1.12. The liquid in the molten zone can be stirred mechanically, or through non-contact methods such as induced electric current. Applied magnetic fields with current passing through the ingot, or high temperature gradients also increase the convective stirring within the molten zone.

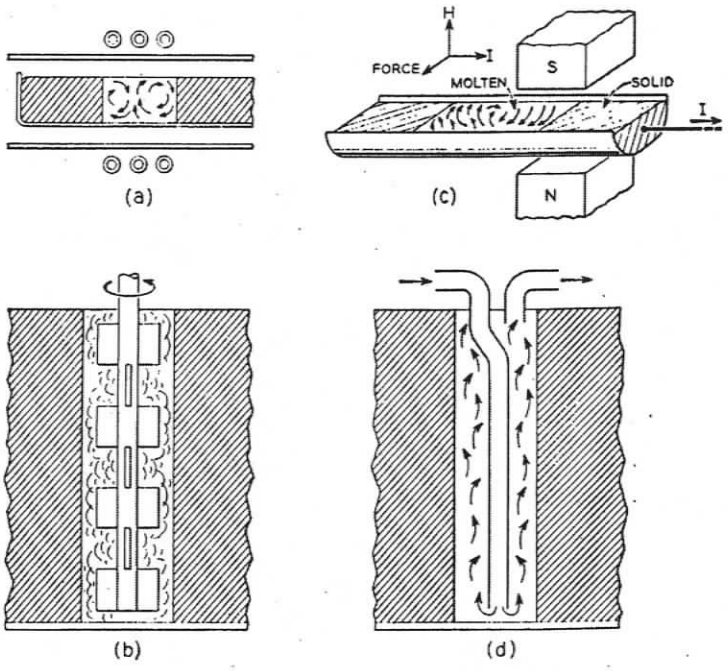

Figure 1.12: Methods of stirring the molten zone; (a) induced current, (b) mechanical, (c) magnetic, (d) pumping the melt [9].

1.3 SIMULATION AND MODELLING

As explained previously, the solute concentration profile after multi-zone refining is much more difficult to calculate than single zone or normal freezing. As a result, numerous electrical, mechanical and liquid analogue simulators have been developed such as the analogue liquid head multi-pass zone refining simulators described in [11].

Numerical models have also been developed for the characterization of the zone refining process and for use in optimization calculations. Theoretical expressions of the distribution after multi-pass zone refining have been made by Lord and Reiss; detailed information on calculating the distribution of multi-pass zone refining can be found in [9]. A short summary of models developed for optimization is given in the following sections.

1.3.1 Optimization

With any given material being zone refined, it is possible to achieve higher purity simply by passing additional molten zones through the ingot (up to the ultimate distribution). Nevertheless, each additional run requires time and results in much higher production costs. In an attempt to increase efficiency, efforts have been made to quantify and optimize the process and equipment in order to reduce the production time and/or cost. Optimization techniques are based on manipulating the effective distribution coefficient and varying zone lengths.

1.3.2 Manipulating the distribution coefficient

The simplest way to increase the efficiency of zone refining is to manipulate the process variables that influence the effective distribution coefficient. It can be seen from the equation for the effective distribution coefficient, (given below) that the zone rate and boundary layer thickness affect k. This is illustrated in the plot of distribution coefficient vs. boundary layer thickness for varied zone speeds given in Figure 1.13.

Effective distribution coefficient: $$k = \frac{1}{1 + (1/k_0 - 1)e^{-f\delta/D}}$$

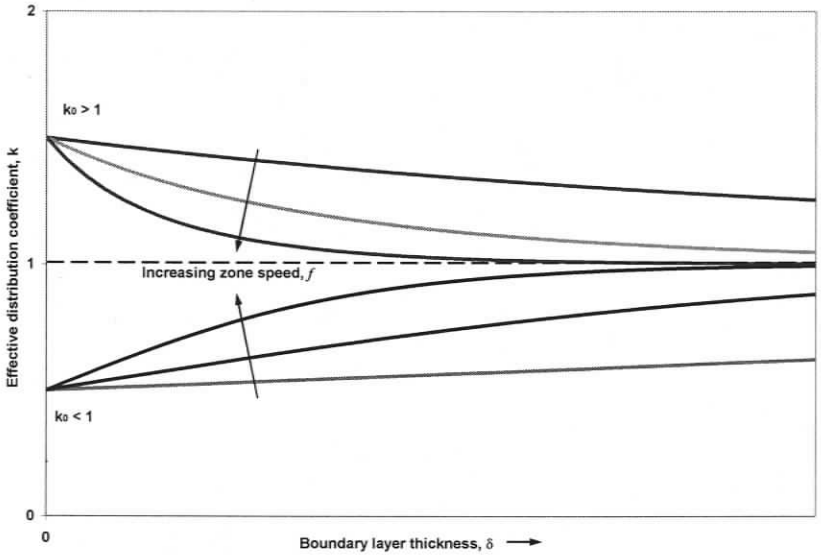

Figure 1.13: Effect of zone speed and boundary layer on *k*.

As seen in Figure 1.13, k approaches unity faster as zone speed and boundary layer thickness increase, resulting in reduced segregation. In order to optimize the process, k must be brought as close to k_0 as possible by reducing the boundary layer thickness and zone travel rate.

While lower zone speeds increase the segregation efficiency (up to the extreme, approaching equilibrium freezing), they result in longer process times or fewer passes per unit time. The time required to achieve a specific purity level varies directly with the number of passes (n) and inversely with the zone speed (f); the ratio n/f for a given k provides a direct measure of this time [9]. When several impurities are involved, the optimal travel rate is determined by the one whose k is closest to unity [9]. A graphical method for determining the value of f which results in the lowest n/f can be found in [9].

Minimizing the boundary layer thickness also increases the segregation of impurities. The boundary layer thickness is directly influenced by the degree of mixing or diffusion in the melt. As outlined previously, mixing can be achieved through mechanical

stirring, or increasing transport within the molten zone by applying a magnetic or electric field. Convection within the molten zone can also be enhanced by a higher gradient due to increased heat input [16]. Trade off between the variables while keeping $f\delta/D$ approximately constant can also decrease production time; e.g. increased mixing allows for higher zone rates.

It has also been shown that the temperature of the molten zone can affect the effective distribution coefficient for some impurities; in general, higher molten zone temperatures reduce the segregation efficiency [19].

1.3.3 ZONE LENGTH

More effective, but more complicated methods of optimization have been developed using varied zone lengths. There have been several different methods in which the optimum zone length has been analyzed. In all of the models presented assumptions were made to simplify calculations such as constant density upon melting, constant distribution coefficient and complete mixing of the molten zone

Rodway and Hunt [15] introduced a method for optimizing zone refining using continuously variable zone lengths. This model optimizes zone refining based on continuously varying the zone length such that the solute concentration in the liquid is equal to that in the solid at the melting interface.

Spim *et. al.* [16] developed a model which utilizes constant optimal zone lengths for successive pass groups, which shows improved refining efficiency to that achieved by Rodway and Hunt.

Ho *et. al.* [17] produced a model that can be used to not only determine the optimum continuously variable zone length (with similar results to Rodway and Hunt),

but also the constant optimal zone length for each pass and constant optimal zone length for all passes. The resulting optimal zone lengths for various k values are given for each of these situations in Figure 1.14. This model concludes that continuously variable zone lengths obtain a higher degree of separation than with constant zones.

Continual variation of the zone gives the best optimization of zone refining, but is likely difficult to implement. Developing equipment for continuously variable zones would be expensive, and control of the zone length difficult to maintain. Proposed methods for controlling the zone size for optimization can be found in [15].

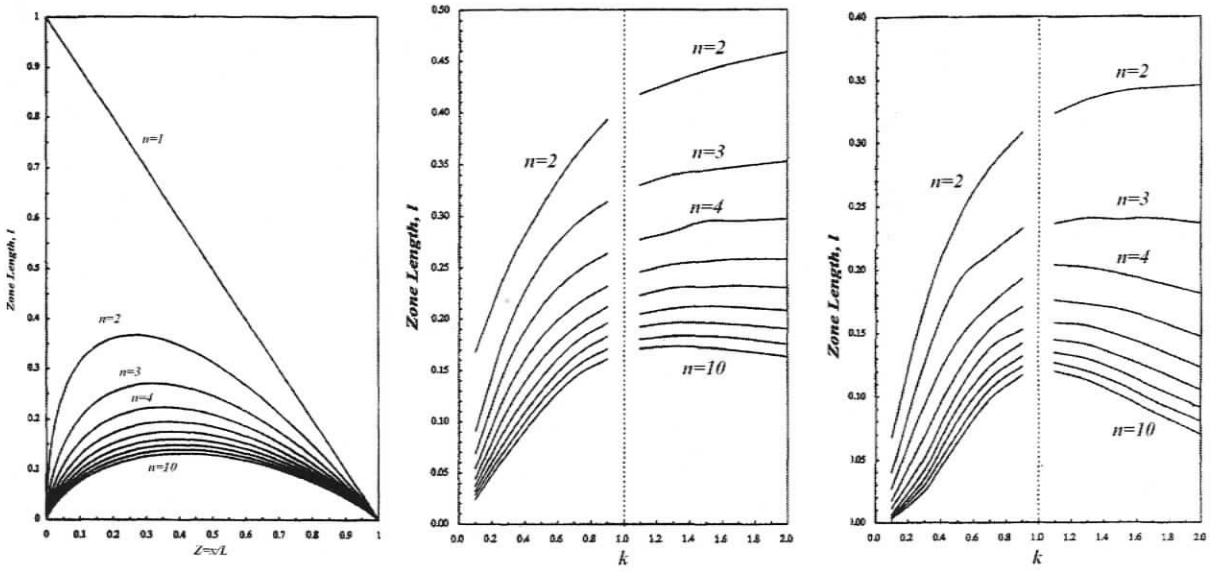

Figure 1.14: Continuously varied optimal zone length (left), constant optimal zone length for all passes (middle) and constant optimal zone length for each pass (right) [11].

In most of the models and simulations researched, there is agreement in some of the fundamental effects of the zone length on segregation. The most significant characteristic of the zone length presented is that longer zones are more efficient for early passes, and shorter zones for later passes [9], [11]-[16]. Long zones favour more rapid

initial purification because as the interface moves, rejected impurity is diluted into a larger volume of material [15]. It has been shown numerous times that the optimal zone length for the first pass is the entire ingot (normal freezing) for all values of k [9], [11]-[16]. The length of the molten zone also affects both the ultimate distribution and the rate at which it is approached; short zones allow much better ultimate distributions to be achieved [16].

It is also generally agreed upon that the optimal zone length increases with the distribution coefficient, but decreases with pass number [11], [17]. This holds true except for continuously varied zone lengths, where it has been shown that there is no dependence on the distribution coefficient [15], [17].

2 ZONE REFINER DEVELOPMENT

This chapter discusses the components and specifications of the experimental zone refiner that has been developed. It then outlines the operation of the system, and explains the testing that has been carried out to date.

2.1 DESIGN REQUIREMENTS

A zone refiner can be constructed in many different ways following one fundamental design requirement: an ingot of material, through which multiple translating zones of different phase are passed. Various methods of heating, containment and travel mechanisms can be used (See [9] [20]-[22]); however, since this project was aimed at increasing the process efficiency of a specific commercial apparatus, the CGL zone refiner had to be similar in design.

The CGL zone refiner has been developed for testing specific optimization parameters as well as validation and comparison with the numerical model. It will also be used for future studies and ongoing research. To provide for the planned testing, and produce practical results, requirements of the design were based on size, number of zones, process variables, and special functionality aimed at the specific testing desired.

The foremost requirement was that the zone refiner must be near production scale. The efficiency of the zone refining process is closely tied to the thermal properties of the system; therefore the scale of the CGL zone refiner had to be close to the current commercial apparatus to give it the same properties. This would also provide for reliable

correlation between the production apparatus and the CGL zone refiner. Although the numerical model should confidently predict any effects of slightly altered production size, larger variations might result in undesirable process differences that would in turn skew any conclusions made from the experimental results.

The zone refiner was also required to operate with multiple molten zones, as a single zone would not realistically represent the middle zones in a multi-zone process. Three zones are adequate; thermal effects in, and operation of the two outside zones are representative of the outside zones in a higher zone process. More importantly, the single middle zone will approximate all of the n-2 middle zones in an n zone refiner. The zone travel rate and zone spacing were also required to be adjustable in order to examine their effect on the process efficiency.

Additionally, the apparatus needed to provide an ultra pure gaseous atmosphere during operation. Capability to apply a vacuum was also required for purging the system.

A few design requirements were intended to accommodate future studies; these were made with the intent of minimizing modifications to the apparatus for later tests. The first of these requirements was the capability to apply a rotating magnetic field around the center molten zone. One of the studies planned is to examine the effect of a rotating magnetic field on mixing in the molten material. The apparatus must be able to provide structural support for electromagnetic coils mounted around the center molten zone (outside of the heater). Another study planned for the zone refiner is electromigration combined with zone refining; in order to test the combined effect, the CGL zone refiner must have the capability to pass an electric current through the ingot (both the solid and liquid zones) during operation.

2.2 CGL ZONE REFINER

The CGL apparatus is a three zone, multi-pass zone refiner, with fixed heaters and a translating charge. It is similar in scale to the commercial system, but with fewer zones to reduce the overall length of the apparatus and keep material costs reasonable. The zone refiner has the capability to adjust all of the typical process variables in order to achieve the most efficient possible combination such as zone speed, zone spacing and number of zone passes. It also has the capability to accommodate the planned studies aimed at increasing the efficiency of the process using an electric current or rotating magnetic field.

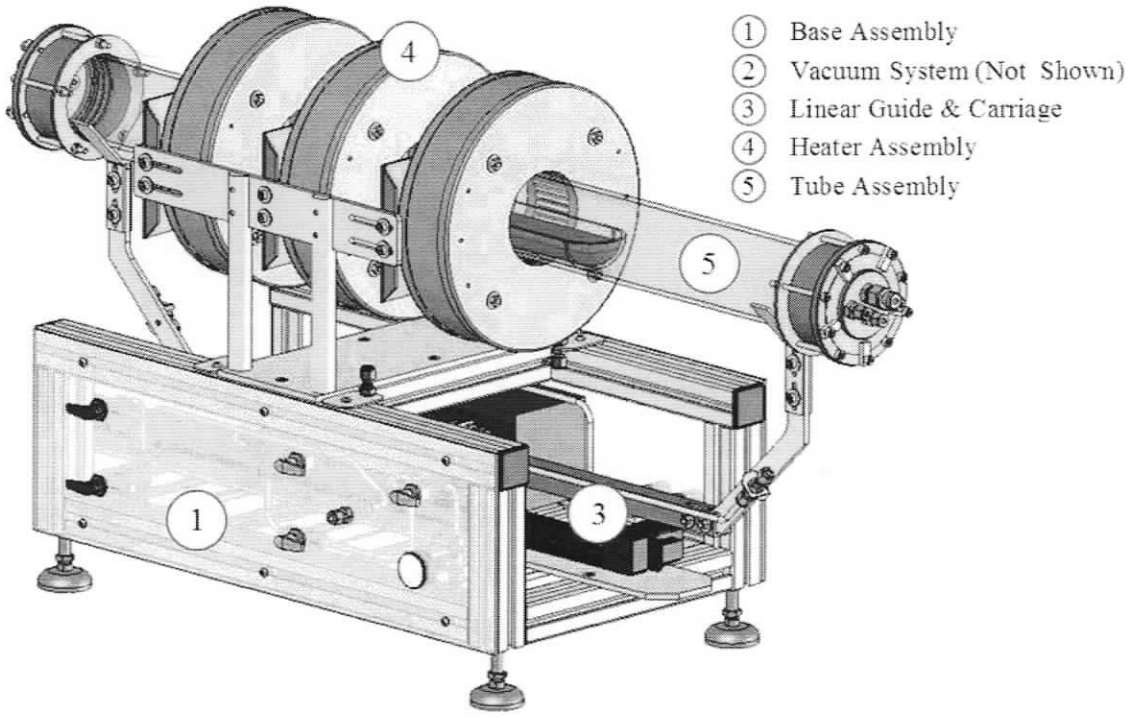

Figure 2.1: Zone refiner CAD model.

The CGL zone refiner can be divided into 5 main components as shown in Figure 2.1: base assembly, vacuum system, linear guide and carriage, heater assembly and tube assembly; each of these is described in the subsequent sections. Many of the specific component details are not included in this document due a confidentiality agreement with 5NPlus Inc.

2.2.1 Base Assembly

The base assembly was built from 45mm x 45mm extruded aluminum tubing for flexibility, its capability for modular assembly and ease of manufacture. It provides a solid structural framework and mounting platform for the entire system which allows the assembly to accommodate heavier loads as may be required in future studies.

A simple on-board gas control system was built into the base to allow the zone refiner to be purged with high purity gas (Figure 2.2). The system consists entirely of stainless steel tubing, fittings and valves to reduce the possibility of contamination. The semiconductor industry has set 316L stainless steel as the standard for the majority of gas delivery applications [28]; although it is more cost effective, brass tubing is a source of contamination, particularly of copper. During operation the system provides a gaseous flow which maintains a highly pure atmosphere. All tubing and fittings in the gas system are rated to 100psi or above, much higher than the maximum operating pressure of approximately 15psi. Brass valves and tubing were also installed in the base assembly for the application and control of water cooling if required.

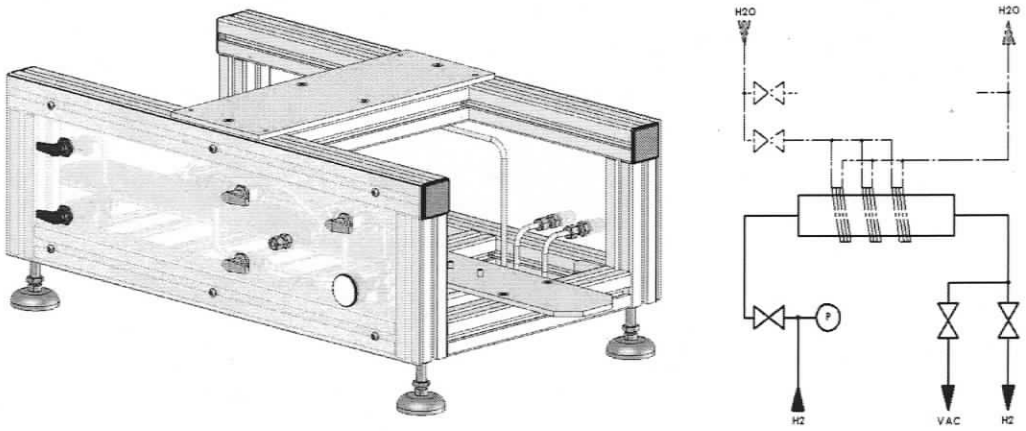

Figure 2.2: Zone refiner base CAD model (left), gas and water schematic (right).

2.2.2 VACUUM SYSTEM

A vacuum system was assembled and connected to the zone refiner to evacuate the tube and gas lines. The vacuum system consists of roughing and turbo-molecular pumps, and a digital vacuum pressure gauge and read-out. The pumps are capable of producing a vacuum of up to 10^{-3} Torr in the zone refiner. The combined vacuum and gas systems give the zone refiner the capability to remove outside airborne contaminants, purge the system with high purity gas, and operate within a clean environment.

2.2.3 LINEAR GUIDE AND CARRIAGE

A packaged linear system was purchased to provide the translation of the charge material through the heaters. The system consists of a precision linear guide with roller bearing carriage, 50Ncm stepper motor, motor controller and software. Translation of the charge is achieved using simple English language programming in the supplied software, which allows for variable zone speeds and precision position control.

This particular system was chosen based on the desired travel length, the load capacity and cost. Calculations of the forces and moments applied to the guide carriage were made using the CAD model weight properties.

As initial testing of the linear system showed that the movement was too coarse at low speeds, the system required a gear reducer to achieve the low speeds needed for zone refining. The gear reducer installed included a 100:1 planetary gear head, along with a replacement bearing and pulley.

Weight was a critical design issue for the dynamic components of the zone refiner due to the load limitations of the linear system. These restrictions required that the tube assembly and support carriage must be lightweight, because a relatively large charge mass was desired. Since the size and material of the tube were predetermined from the commercial apparatus, the only parts remaining that could influence the overall weight were the tube carriage and end caps. Calculations were made in order to ensure that the tube carriage was rigid enough to support the charge material and tube assembly while staying within the load capability of the linear guide and stepper motor. General stress/strain as well as numerical calculations were carried out for critical components.

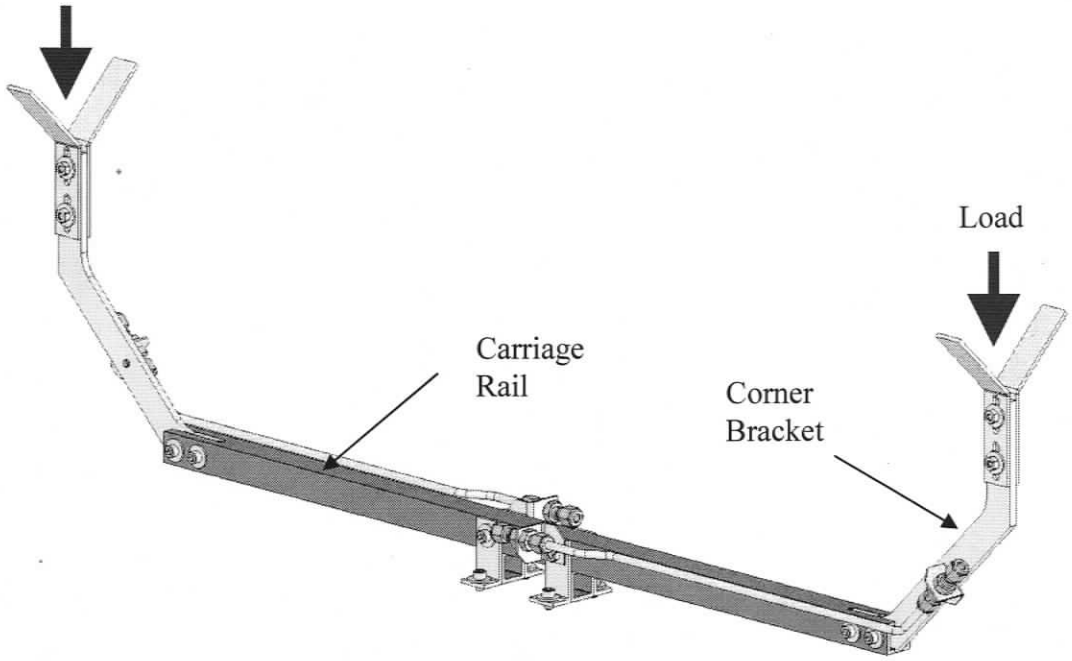

Figure 2.3: Tube carriage CAD model.

Calculations were made on the corner bracket and carriage rail to determine their associated stresses and deflections. The load calculations on the corner bracket showed maximum stress on the order of 18MPa, resulting in a safety factor of approximately 15. Calculations carried out on the carriage rail determined the maximum stress to be around 26MPa; a safety factor of 11. Finite element analysis (FEA) was carried out using COSMOS software to verify the calculations. The FEA analysis showed very localized stress concentrations as a result of the geometry required for defining the load and support surfaces. These geometries were not part of the original components, so the localized stresses at these locations were not realistic. Neglecting these localized stress concentrations projected by the model, the FEA results were in agreement with the calculations (See Figure 2.4 and Figure 2.5). Some flexibility of the carriage was accepted as a trade-off for reduced weight. The analysis showed that the rail would flex

approximately 1.7mm when loaded; an acceptable amount given the adjustability incorporated into the system.

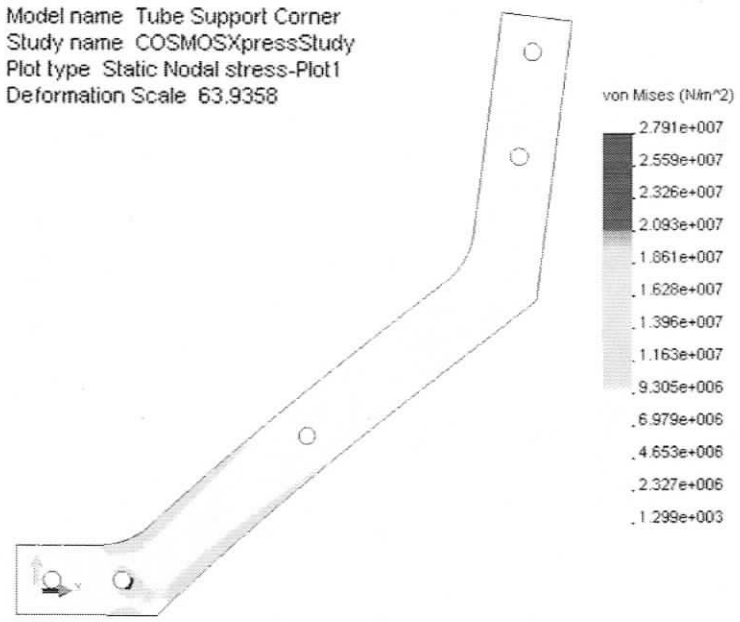

Figure 2.4: Corner bracket FEA results.

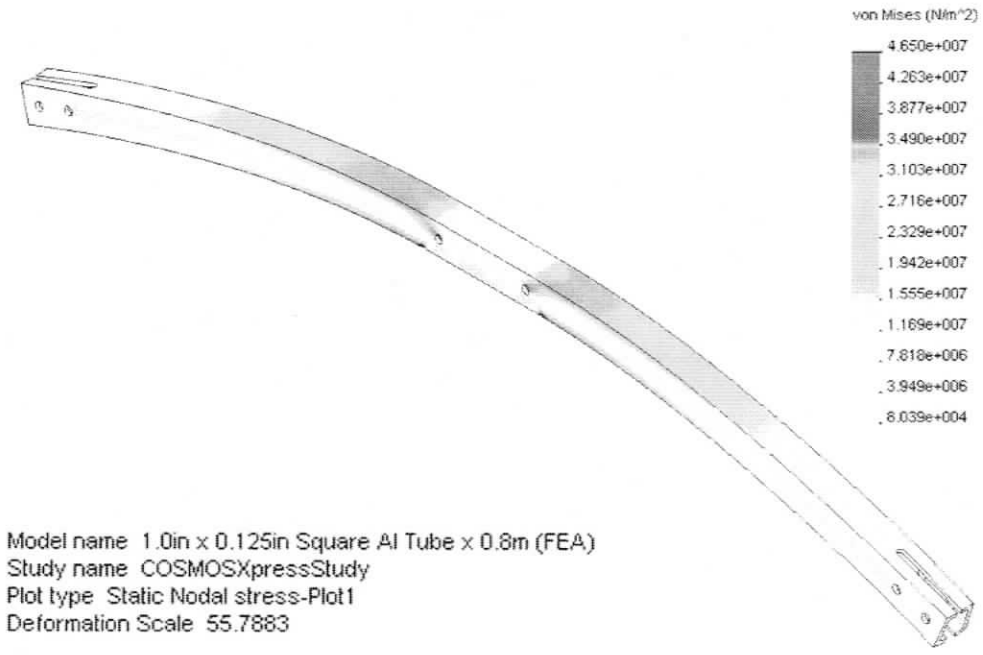

Figure 2.5: Carriage rail FEA results.

2.2.4 HEATER ASSEMBLY

For accurate correlation with the commercial apparatus, resistance heaters similar to those used in the commercial apparatus were acquired for use in the CGL zone refiner (the only difference between the CGL and commercial heaters being the location of the electrical junction box). Thermocouples were installed into the heaters for monitoring the temperature and for control feedback. They were placed such that they protruded through the heater to the inside of the inner heater ring near the upper tube surface. An integrated power supply and controller was utilized with each heater. The controllers were chosen for this application based on their price, power output, available control functions, and that they did not require external power supplies. The controllers have the capability for PID temperature control and ramp/soak profile programming of the heaters up to their maximum rated power.

2.2.5 TUBE ASSEMBLY

The CGL zone refiner utilizes a high purity quartz tube built from the same diameter tubing as the commercial apparatus; this allows the use of the existing commercial heaters and results in "at scale" testing. To contain the charge material, a quartz boat is used; it is the same diameter as the boats used in production, only shorter to fit the CGL zone refiner. The geometry of the boat is shown in Figure 2.6.

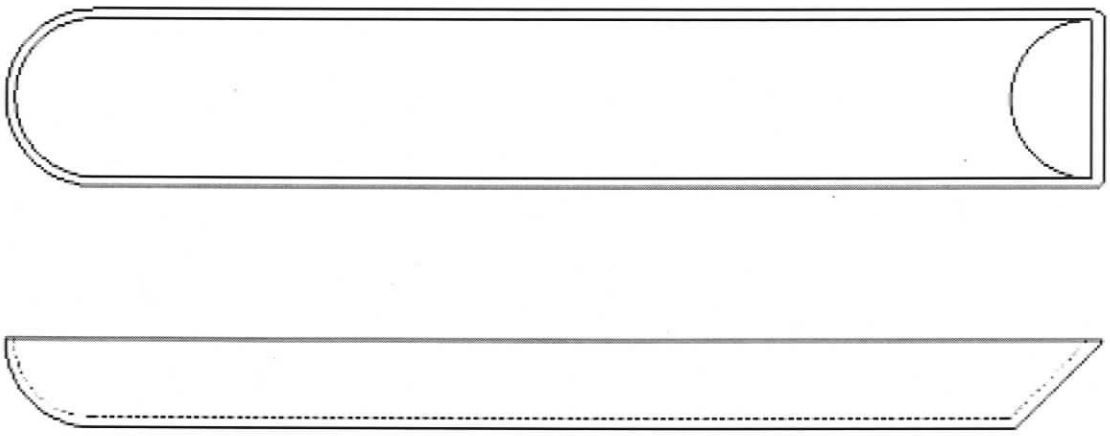

Figure 2.6: Quartz boat geometry.

End caps for the tube were designed based on functionality and weight considerations; they integrate pressure sealing, process gas connections, electrical feed-through and access to the charge. All of the parts in contact with the process were manufactured from stainless steel to avoid introducing contaminants.

Frequent access inside the tube is required for removal of the charge and cleaning. This is achieved via a removable flange sealed with a face seal o-ring. This access flange eliminates the need to remove and install the end cap before each experiment, reducing handling of the quartz tube, and thereby reducing the possibility of breakage.

For the proposed experiments using electromigration, a pressure sealed pass through fitting was included in the end caps for passing a current rod through to the charge material. Spare ports were also included for thermocouple access if needed.

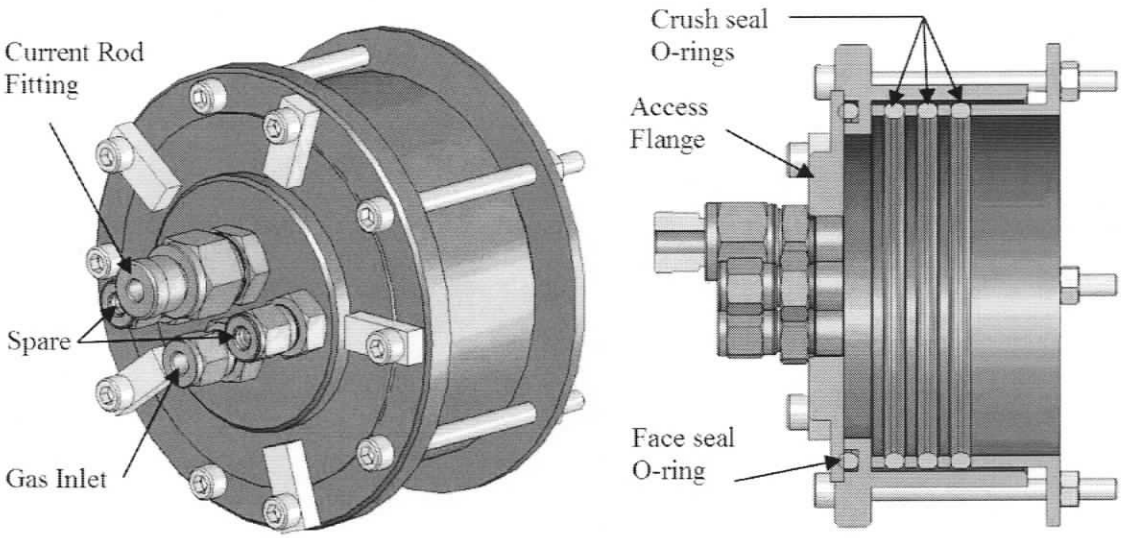

Figure 2.7: End cap assembly and cross-section.

The end caps make use of o-ring crush seals for both sealing between the tube and end caps as well as mechanically fastening the end cap to the tube. Three silicone o-rings are pressed between three stainless steel back-up rings by a flange (See Figure 2.8), as the o-rings are pressed they expand against the tube and end cap. This pressure provides a seal between the process gas inside the tube and the outside air; friction between the o-rings, the tube and the end caps keep the assembly securely fastened.

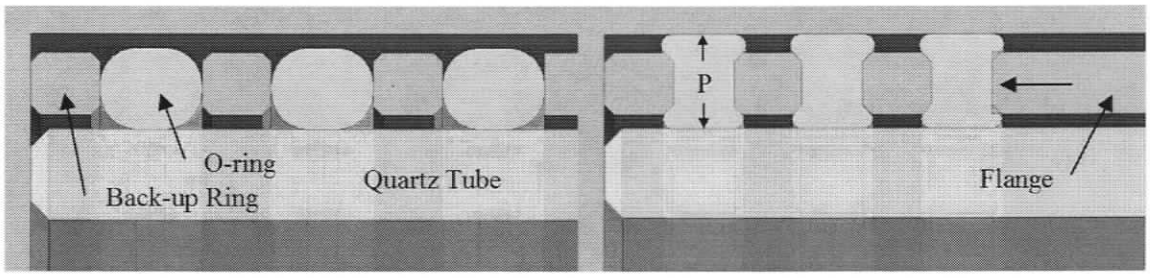

Figure 2.8: O-ring crush seal, before (left) and after assembly (right).

2.3 VALIDATION TESTING

Once the design and assembly of the CGL zone refiner system was completed, a series of tests were carried out to prove and characterize the system. The gas system (minus the tube) was pressure tested to 30psi using nitrogen gas to check for leaks; the tube was not included in this pressure test due a lower pressure rating of the end cap seal. The tube was designed to operate at approximately 3psi pressure under normal conditions; it was tested for leaks under 15psi pressure. After the heaters were installed and connected to the controllers, a "bake-out" was carried out to check their operation and remove moisture from the heater insulation. The PID (proportional, integral, derivative) values which gave the best control of each heater were determined using the controllers' auto-tune function.

2.3.1 THERMAL TESTING

Thermal testing was initiated in order to determine the temperature set-points required for various steps in the process, and the heaters' ramping capability. Individual segments of the zone refining process were also run to ensure that each portion would perform as desired.

All of the experiments were conducted using tellurium. Tellurium is an important semiconductor material; it is used in semiconductor compounds such as cadmium telluride (CdTe), cadmium zinc telluride (CdZnTe) and cadmium mercury telluride (CdHgTe), which form the active elements in sensitive infrared detectors for thermal imaging, x-ray and gamma-ray detectors, night vision equipment, and solar cells among others [3],[24]. Tellurium was chosen because it is a relatively easy material to purify

using zone refining. The combination of its lower thermal conductivity, 2W/mK [29], and moderate melting temperature 449.5°C [29] facilitates cooling between zones; this makes it relatively easy to generate and maintain separate molten zones.

First, an experiment was conducted to determine the system specific temperature set-points and times required to melt, and subsequently to solidify the ingot. To this extent the heaters were ramped up until the charge melted, and the time to melt recorded; similarly for the solidification. Secondly, the set-points and times required for the formation of separate zones were ascertained, followed by the set-points for control of dynamic zones. These were determined by forming zones, translating the ingot and adjusting the heater temperatures as required. Different set-points were tested to determine the stability of the molten zones with varied temperatures in both the static and dynamic tests. Finally, an experiment to make certain that the molten zone was maintained during the "fast" return movement of the charge between heaters was conducted; the zones were transferred between heaters at 15mm/s to ensure that they did not begin to solidify and that they were located properly.

Once the above tests were concluded, a temperature and timing profile was designed for the heaters that would subsequently melt, solidify and then form separate molten zones in the ingot for purification. This profile was tested to ensure that the temperature set-points and timing were adequate for fully melting the charge, forming an ingot and then stable zone formation.

An additional experiment was conducted to ensure that the first heater was able to form a molten zone at the leading edge of the solid ingot. Unlike at the second and third heater, upon starting translation, the charge material at the first heater would not already

be molten; therefore the temperature within the first heater had to be sufficient enough to melt the charge as it was passed into the heater. As a result of this test, slight modifications had to be made to the heater profile described above. A final experiment was then conducted to melt, cool and form zones in the ingot to verify the modified heater profile.

Table 2.1: Thermal and verification tests conducted

Test	Objective
A	Determine the temperature set-points required to melt the entire ingot; record the time required for the heater ramp up to the set point and time for the entire ingot to melt.
B	Determine the temperature set-point and the time required to form separate molten zones in each heater. Adjust the SP and determine the stability and size of the zone relative to temperature.
C	Ensure that the zones are properly positioned and the heater is able to capture the molten zones after the fast return translation.
D	Test the ramping profile and timing (developed based on SP and timing determined above) to ensure that it is able to consecutively melt, solidify, then form separate zones in the ingot.
E	Ensure that the first heater is able to form a zone from the solid ingot as it is passed through.
F	Test the modified ramp-up profile

2.3.2 THREE ZONE PASS PURIFICATION TESTS

Once confidence in the system's operation had been attained, full process tests could be initiated. A series of three-zone pass tests were performed and samples removed from the purified ingots; three samples from the third and eighth experiments were sent for glow discharge mass spectrometry (GDMS) analysis. The apparatus was supervised closely during the first full process experiment to ensure that it operated correctly, but during later tests it was left to run on its own.

2.4 OPERATION

2.4.1 MATERIALS HANDLING

Before assembling the zone refiner, the quartz pieces were etched; the tube in HNO_3, the boat in 1:3 HNO_3:HCl (aqua regia). All handling of the charge materials was carried out in the CGL cleanroom with material-specific containers and tools to avoid contamination. The charge material was kept in a clean environment at all times while inside the zone refiner, even when an experiment was not in progress. The ultra-high purity gas used in the zone refiner was supplied from bottles via the CGL lab gas system.

When an experiment was complete, the ingot was kept under a flux of gas and allowed to cool to room temperature before exposure to the outside air. Once cooled, the purified ingot was removed from the zone refiner and transferred to the cleanroom for processing. The ingot was weighed, photographed, and its properties recorded. Samples were removed from the ingot from pre-designated locations (See Section 2.4.4), and then the ingot was broken into small chunks which allowed it to be re-loaded into the boat.

The material was exposed to the open air for as little a duration as possible to minimize oxidation. When not running an experiment, the material was placed in the clean environment of the zone refiner tube, or stored in a vacuumed-sealed bag. After each experiment, condensed charge material and impurities were found on the inside of the tube, boat and end caps; those components were thoroughly cleaned of all residual material with methanol before the zone refiner was reloaded.

2.4.2 CHARGING THE SYSTEM

To load the system, ingot pieces were evenly placed along the length of the boat. Additional source material was added to produce a 3kg total charge; this was necessary since a reduction of approximately 40-50g in the ingot's mass incurred due to handling and evaporation during operation. The boat was positioned inside the tube such that it was centered in the heaters, then the tube sealed at the end caps, and a vacuum applied to evacuate air. Next, the system was purged with gas and a low pressure flow initiated through the system.

2.4.3 ZONE PURIFICATION PROGRAM

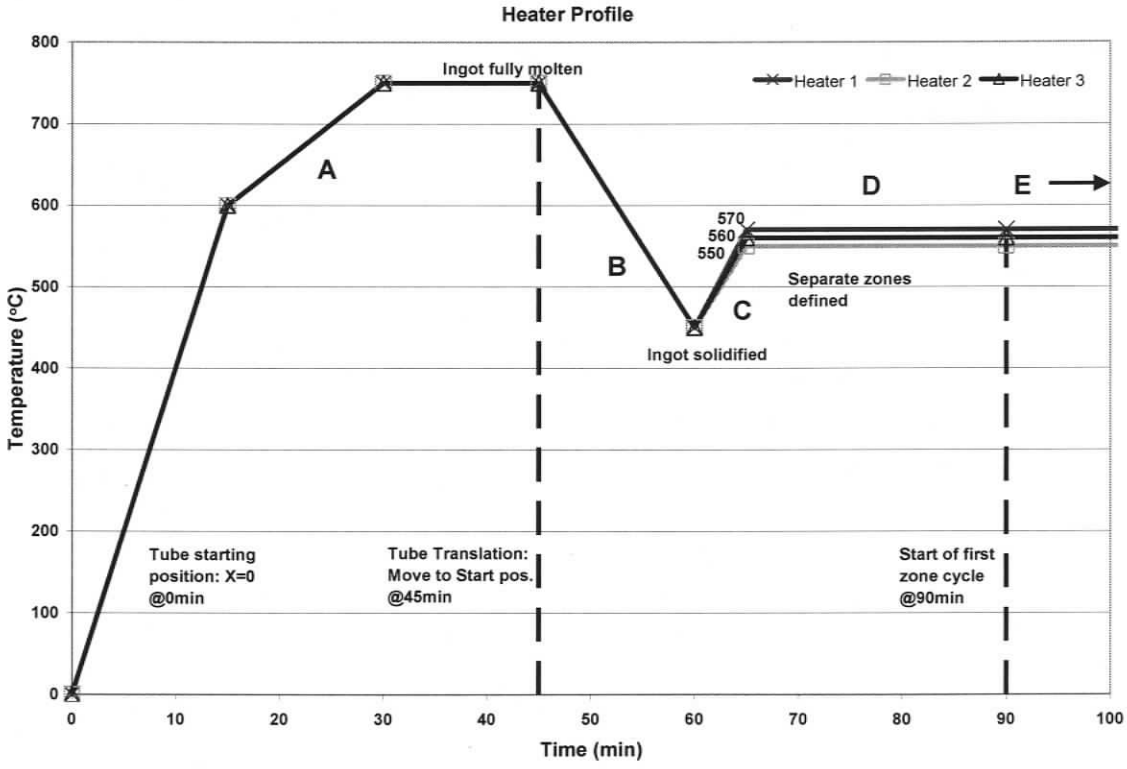

Figure 2.9: Heater temperature and timing profile.

Before starting the purification process, the entire charge was melted, and then cooled, to form a solid ingot. Once the material solidified, separate molten zones could be formed. When stable, the charge was translated at the desired rate with the separate molten zones being translated along the ingot in one direction. The heater temperature and timing profile that provided the functions described above is given in Figure 2.9; the profile can be divided roughly into five sections, labelled A to E.

The sequence was initiated by the ramping up of the heaters to melt the charge material. All three heaters were quickly ramped up to 600°C then 750°C over 30 minutes and held at 750°C for 15min. Next, the heaters were ramped down to 450°C over 15min to allow the charge material to solidify into a single solid ingot. At the initiation of the ramp down, the tube was moved to the zone cycle starting position (1/2 the heater spacing from the central position). Once the charge material solidified, the heaters were ramped back up to their zone operating temperatures (heater #1 ≈ 570°C, heater #2 ≈ 550°C, heater #3 ≈ 560°C); and maintained there for 25min prior to the start of the first zone pass in order to stabilize the zones. The heaters were then set to maintain their respective operating set points for the remainder of the process; each heater was turned off in sequence once the n^{th} pass had been carried through.

The linear system controller initiated translation of the tube once the zones were established; an example of the heater movements required for translating molten zones using multiple heaters is given in Figure 2.10 (In the figure, the heaters are translated and the tube static to better show the relative movement; on the CGL zone refiner the heaters are fixed and the tube translated). First, the tube was slowly translated at the desired rate the distance of one heater spacing (See Figure 2.10a to c). Once the tube reached the end

of this movement, it was returned quickly back to the start position at 15mm/s (Figure 2.10c to a). The molten zone left by one heater (H1) was recaptured by the heater in front of it (H2). Slow translation was started again after a two minute pause, which ensured that the zones remained stable after being transferred between heaters.

This translation-return reciprocating heater cycle was repeated n+2 times in order to pass n complete zones through the ingot. The process control schematic for passing three complete zones with the CGL zone refiner is given in Figure 2.11. While the two partial zone passes at the beginning of the process (n = -1, n = 0) contributed to the purification of the ingot, they were not counted as full zone passes.

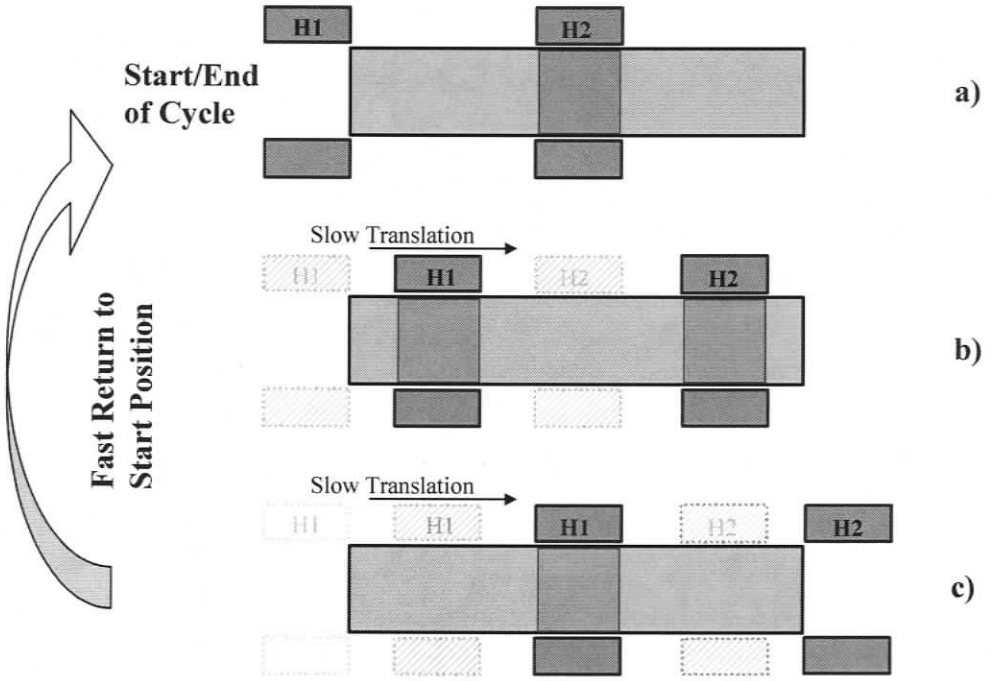

Figure 2.10: Heater cycle and zone movement diagram for passing zones with two heaters (H1, H2).

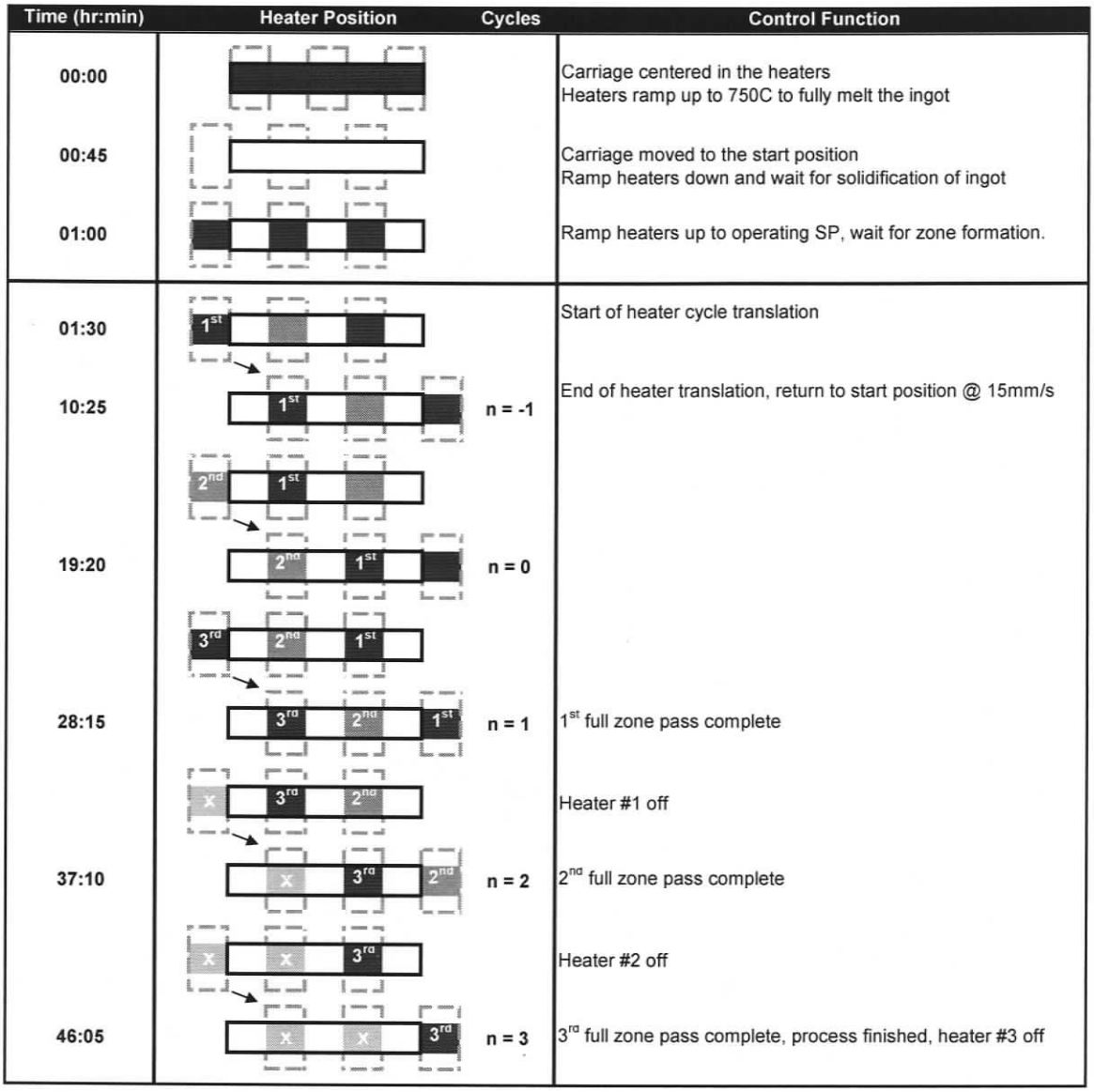

Figure 2.11: Zone refiner control schematic (shown for 3 zone passes).

Operation of the system was handled automatically by the heater controllers and the motion control software. The heaters were pre-programmed with the ramp up/down profile as required to melt, solidify and then generate zones in the ingot. The linear system was programmed to start movement of the tube and timed to correspond with the heater sequence. Once the system had been started (heater and motion controllers) no further operator input was required.

2.4.4 SAMPLING

Samples were removed from the ingot after each experiment. The samples were taken from the tip and tail of the ingot, as well as equally along the length at approximately every 75mm. Samples were removed from as near to the center of the ingot as possible; the exact position was affected by the material grain structure as it was much more difficult to break across the grain and often hard to extract a sample from an exact position. The samples were vacuum sealed in plastic bags and selected ones sent for GDMS analysis by the Chemical Metrology Group at the National Research Council of Canada Institute for National Measurement Standards. Samples that were not sent for analysis were stored and documented in the CGL lab for future reference as needed.

3 EXPERIMENTAL RESULTS

The results of the experiments carried out are reviewed in this chapter. The method of analysis is briefly discussed and conclusions made based on the analysis data.

3.1.1 THERMAL TESTING

The required temperature set-points and timing were determined from the initial thermal testing without major difficulty. Using these values, a heater ramp-up profile was created that reliably melted the charge, solidified it into a solid ingot and then formed separate molten zones as desired. The molten zones were found to be very stable; the zone size remained consistent when held at an appropriate set-point of approximately 570°C for heater #1, 550°C for heater #2 and 560°C for heater #3. It was also found that the size of the molten zone could be influenced by adjusting the heater set-point by approximately 10°C increments.

3.1.2 THREE ZONE PASS PURIFICATION TESTS

Table 3.1 presents the GDMS data indicating the residual impurities in the three samples tested from the third and eighth three zone pass experiments; the concentrations from the two tests are illustrated in Figure 3.1 and Figure 3.2 respectively. GDMS results from the source material are included for comparison. Both a partial and full analysis were carried out on the source material, which gave results that illustrated the accuracy of

the GDMS analysis. Financial considerations prevented GDMS analysis of samples from all experiments.

Table 3.1: GDMS results for three zone pass experiments #3 and #8.

Institute for National Measurement Standards Chemical Metrology						Glow Discharge Mass Spectrometric Report ppb (Atomic)		
	Te Source		Test #3 Samples			Test #8 Samples		
Element	Partial	Full	Tip	Middle	Tail	Tip	Middle	Tail
Li		<6	<9	<8	<9	<8	<7	<12
Be	<14	<5	<7	<7	<8	<7	<6	<8
B	<7	<6	<7	<7	<5	<6	<5	<9
C		950	29	36	43	450	290	700
N		280	4	4	5	55	45	80
O		1300	57	56	20	980	580	1000
F		<25	<20	<15	<10	<20	<15	<50
Na	83	<4	<5	<5	<5	<4	<4	<7
Mg	<7	<3	<4	<4	<3	<3	<3	<5
Al	26	<2	<2	<2	<2	<2	<2	12
Si	30	25	<3	8	21	<5	<7	15
P		<3	<4	<4	<3	<3	<3	<5
S	<20	<7	<4	<4	<4	<6	<5	<6
Cl		<7	<3	<3	<2	<5	<6	<8
K		<30	<10	<10	<8	<15	<15	<20
Ca	<95	<35	<30	<25	<20	<65	<45	<80
Sc		<0.9	<1	<1	<1	<2	<1	<2
Ti	9	<0.5	<0.7	<0.6	<0.4	<0.5	<0.5	<0.9
V	<0.8	<0.3	<0.5	<0.4	<0.5	<0.4	<0.4	<0.5
Cr	<3	<2	<2	<1	<2	<3	<2	<2
Mn	<2	<0.9	<1	<1	<1	<1	<1	<1
Fe	<5	<0.8	<0.7	3	<0.7	<0.7	<1	<1
Co		<0.5	<0.7	<0.7	<0.8	<0.7	<0.6	<0.7
Ni	<3	<1	<2	<2	<2	<2	<2	<2
Cu	<7	<3	<4	<5	12	<4	<3	<4
Zn	<18	<8	<11	<10	<11	<10	<9	<12
Ga	<7	<3	<4	<4	<4	<4	<3	<4
Ge	<14	<6	<8	<6	<9	<8	<7	<9
As	<4	<2	<2	<2	<3	<2	<2	<3
Se	<50	<10	<10	<10	<10	<10	<10	<10
Br								
Rb		<1	<2	<2	<2	<2	<1	<2
Sr		<0.6	<0.8	<0.8	<0.9	<0.8	<0.7	<1
Y		<0.5	<0.7	<0.6	<0.7	<0.7	<0.6	<0.8
Zr	<1	<0.5	<0.7	<0.7	<0.7	<0.7	<0.6	<0.8
Nb		<0.4	<0.6	<0.6	<0.6	<0.6	<0.5	<0.7
Mo	<2	<1	<1	<1	<1	<1	<1	<2
Pd								
Ag	<8	<3	<5	<5	<5	<5	<4	<6
Cd	<20	<8	<12	<11	<12	<9	<10	<13
In	<3	<1	<2	<2	<2	<2	<1	<2
Sn	<10	<4	<6	<6	<7	<9	<8	<8
Sb	<130	<30	<60	<95	<55	<85	<100	<80
Te	Matrix	Matrix	Matrix	Matrix	Matrix	Matrix	Matrix	Matrix
I		<550	<670	<860	<630	<950	<1000	<870
Cs		<3	<9	<9	<8	<10	<8	<8
Ba		<3	<4	<4	<3	<3	<3	<3
La		<0.4	<0.3	<0.2	<0.2	<0.7	<0.2	<0.3
Ce		<3	<0.6	<0.3	<0.2	<0.7	<0.3	<0.9
Hf		<0.6	<0.8	<0.8	<0.8	<0.8	<0.7	<0.9
Ta								
W		<0.8	<1	<1	<1	<1	<0.9	<1
Pt		<3	<4	<4	<4	<4	<3	<5
Au	<65	<10	<10	<10	<10	<10	<10	<10
Hg	<17	<4	<6	<5	<6	<5	<4	<6
Tl	<4	<2	<2	<1	<2	<2	<2	<3
Pb	<1	<0.7	<0.8	<0.7	<0.8	<0.6	<0.6	<0.8
Bi	<2	<0.5	<1	<1	<1	<1	<0.8	<1
Th		<0.2	<0.2	<0.2	<0.2	<0.2	<0.2	<0.2
U		<0.2	<0.2	<0.2	<0.2	<0.2	<0.2	<0.1

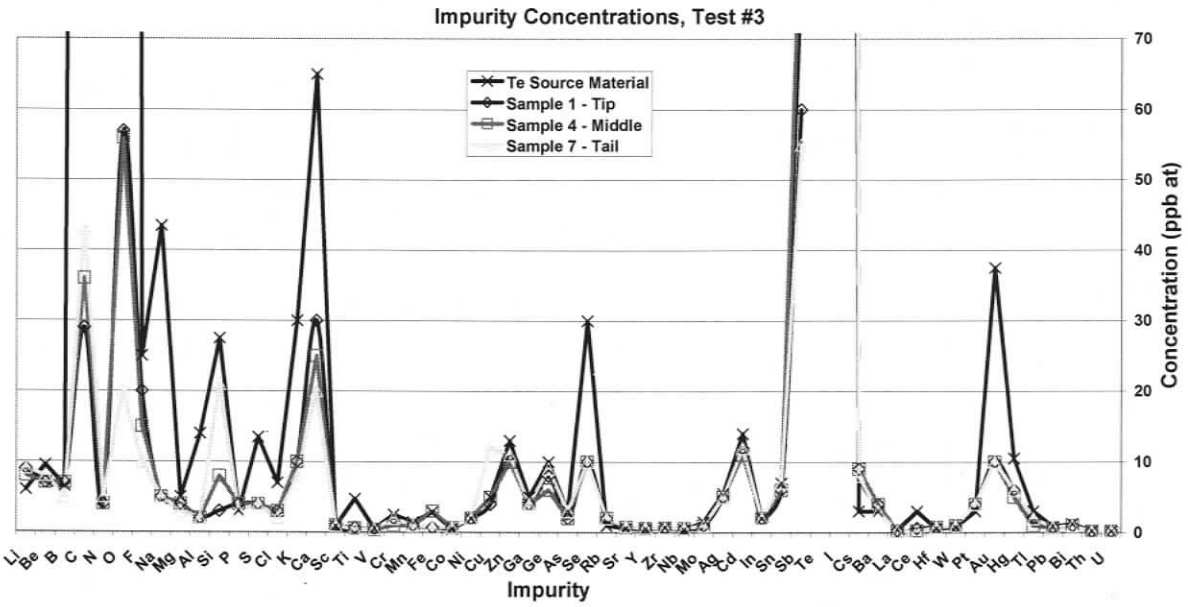

Figure 3.1: Impurity concentrations after the 3rd three zone pass experiment.

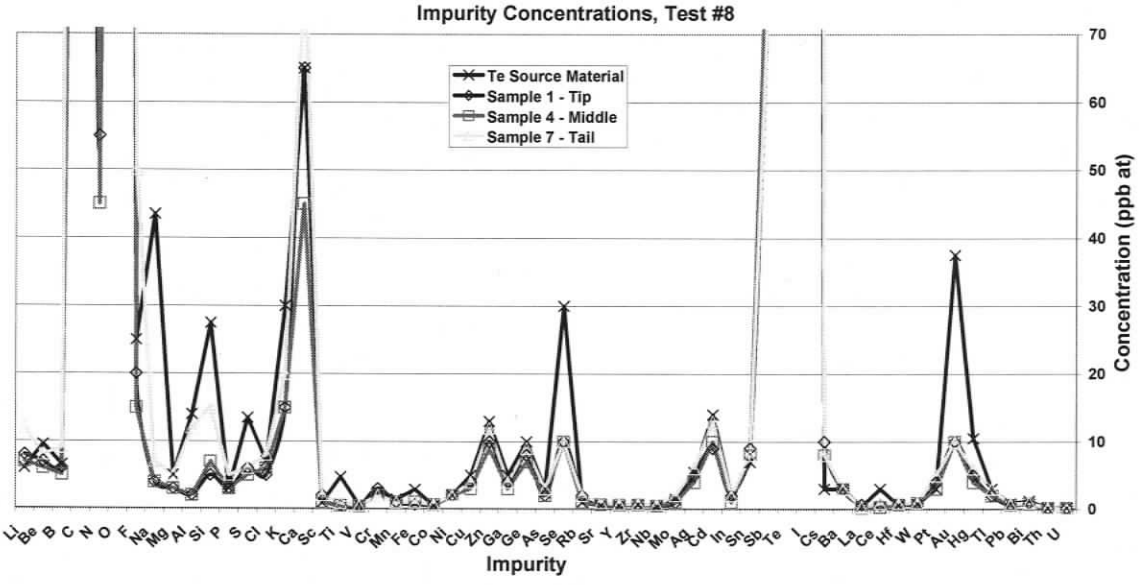

Figure 3.2: Impurity concentrations after the 8th three zone pass experiment.

The "less than" in Table 3.1 indicates the maximum concentration level; it is probable that the actual concentration is lower, but it is impossible to distinguish the specific element given the GDMS output. This is due to reduced visibility of the individual mass readings correlating to the target element either from noise due to interaction with the surrounding physical environment or elemental compounds. At such low concentrations, it is difficult to determine the exact level of impurities given the GDMS accuracy; a consequence of this is the inability to make definite conclusions on the purification efficiency with respect to many of the impurities.

The objective of analyzing samples from the two ingots was to determine if the apparatus was operating as desired, that is if purification of the material occurred, and if any impurities were introduced during the process. If an impurity were introduced during handling or zone refining, a significant increase in the impurity concentration would be seen after running multiple experiments. However, in general a reduction in concentration was observed for all impurities tested with no unexpected spikes in concentration. Because of this, it can be concluded that there were no external sources of contamination from the CGL process.

The GDMS data in Table 3.1 also shows that the CGL zone refiner is capable of purifying an ingot of tellurium even with as few as three full zone passes; there was definite removal of many of the impurities. There were exceptionally low concentrations of carbon, nitrogen and oxygen in the purified ingot from the third test compared to the source material; these values obtained with the CGL zone refiner were even significantly lower than those attainable using the commercial apparatus. It is unclear exactly why the CGL zone refiner was considerably more efficient at removing the C, N and O during this

experiment. The residual concentrations of C, N and O in the ingot from the eighth test were at a level more representative of the commercial apparatus's capability.

Most of the impurities in the ingots appeared in very low residual concentrations; the readings were too low to distinguish any concentration profile along the ingot. However, the level of a few impurities remained high enough to produce a concentration profile. Some elements from the third test such as silicon (See Figure 3.3a) showed a concentration profile after the three zone passes that indicated it has a distribution coefficient <1; the greatest reduction in concentration was at the tip of the ingot. Other elements such as oxygen (See Figure 3.3b) (also possibly fluorine and calcium) showed a concentration profile that indicated it has a distribution coefficient >1; the greatest reduction in concentration was at the tail of the ingot.

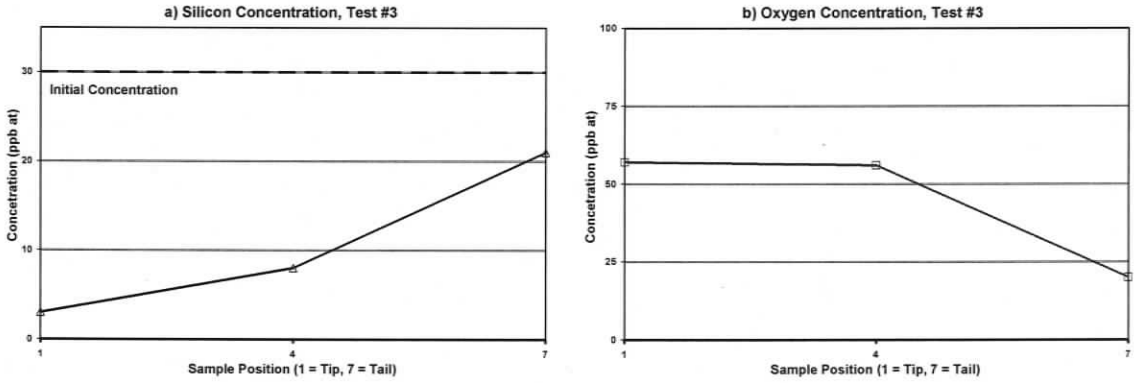

Figure 3.3: Residual Silicon and Calcium concentration profiles after 3 zone passes.

The largest impurity concentration was associated with iodine; however it is uncertain if the reading is from the elemental form, compounds or noise associated with the matrix element tellurium. The source material also showed high iodine and antimony concentrations and it is suspected that these high readings are due to their close vicinity in atomic mass to that of tellurium. An unexpected anomaly in the data was the lack of a

peak in concentrations at the extremes of the ingot, i.e. the tip and tail. Upon purification, the impurities should be concentrated in these ends and the residual concentration should be higher than that of the source material. One possible reason for the anomaly is the location from which the tip and tail samples were taken; samples were removed from the interior of the ingot only i.e. no material from the upper face or from the surface in contact with the quartz was sent for analysis.

4 ONGOING WORK AND FUTURE STUDIES

This chapter provides an overview of the experimental studies planned for the CGL zone refiner. It also outlines recommended improvements to the system.

4.1 OPTIMIZATION STUDIES

Using the CGL zone refiner, tests will be carried out to determine the effect on the purification efficiency using specific techniques and varying process variables. Methods will be tested that would most likely increase the efficiency (increase purity or decrease production time) based on theory and recommendations from the numerical study.

4.1.1 IMPURITY CONCENTRATION

In order to determine any effect of modifications to the apparatus on purification efficiency, a dopant will need to be added to the charge material. Although the GDMS results are relatively accurate and repeatable for some impurities at low concentrations, they possess large statistical errors associated with the GDMS technique. The low levels of residual impurities obtained with the CGL zone refiner are smaller than the presented GDMS errors; a dopant will be used to ensure that the residual concentration of a single impurity will be higher than the error and no variation in concentration is a result of the GDMS readings.

The initial quantity of dopant required can be calculated from its effective distribution coefficient, the number of zone passes and the desired final concentration

(approximately 200ppb or greater to confidently exceed the GDMS error). Before running an experiment with the doped charge material, samples will be removed from the ingot after it has been solidified. This data will be used to determine the distribution of the dopant before purification (homogeneous or not) and for comparison with the later purified ingot.

4.1.2 Applied Electric Current

When an electric field is applied to a metal, a small net transport of matter occurs in addition to the flow of electrons; this transport is referred to as electrotransport [30]. It has been shown that the combination of electrotransport with vertical zone refining can improve the purification process [31]; in order to examine the effect of electrotransport on purification in a horizontal system, an electric current will be applied to the CGL zone refiner. Current will be applied to the ingot across two graphite contacts, one located in each end of the ingot; a power supply connected to the graphite rods will be used to drive a current during the experiments. Impurities remaining after these experiments will be compared with the results from the standard zone refining tests to quantify the effect.

4.1.3 Rotating Magnetic Field

It is known that a rotating magnetic field affects mixing in the liquid phase of an electrical conducting melt [32]-[34]. The rotating magnetic field induces an electric field that generates an electric current, which in turn creates Lorenz forces; these forces drive the primary azimuthal flow in the melt (perpendicular to the rotational axis of the magnet) [32]. A significantly smaller secondary cell flow in the axial and radial directions is also generated due to pressure gradients and centrifugal forces [32].

It is felt that the forces generated by the rotating magnetic field will increase the mixing and therefore decrease the boundary layer thickness at the freezing interface of a zone refiner molten zone. Electromagnetic coils have been purchased and are to be placed around the center heater of the CGL zone refiner. Once installed, the effect of the rotating magnetic field on the purification efficiency of the zone refiner will be examined.

4.2 ALTERNATIVE MATERIALS

Testing will also be carried out in the future using cadmium, and possibly zinc, as the charge material. Separate contact and quartz pieces will be utilized and the end caps will be disassembled and thoroughly cleaned to reduce the possibility of contamination. The apparatus will be modified to suit the new material; the zone spacing and translation rate will be adjusted, and the initial thermal testing conducted again to determine the appropriate temperature set-points and timing for each material.

4.3 IMPROVEMENTS TO THE DESIGN

Although the CGL zone refiner has proved to be a reliable and stable apparatus, there are modifications that can be made to improve the process. The first, and most significant modification, is the creation of a combined control program for the linear system and heaters. It would be beneficial to integrate the two systems in order to precisely synchronize the process timing and possibly incorporate data logging capability. A centralized controller could also be set up to pause, continue or shut the system down in case of an error.

Another desired modification is to add a back pressure regulator to the gas outlet of the apparatus; this would allow precise control of both the pressure in and flow through the zone refiner gas system.

5 CONCLUSIONS

The CGL zone refiner was built to accommodate all of the requirements set out for it; it is near production scale, contains multiple zones with variable spacing and translation rate, has the capability to operate under a flowing high purity gas atmosphere and it can accommodate hardware for testing with a rotating magnetic field and electromigration. The apparatus was designed to be a full featured zone refiner. In order to achieve the most efficient possible combination, the zone refiner was developed with the capability to adjust all typical process variables such as zone speed, zone spacing, and number of zone passes, as well as accommodate different methods aimed at increasing the mixing in the melt.

During both initial thermal testing and full three zone pass experiments, the zone refiner performed as expected without difficulty. The entire process has been qualified and determined to be stable and easily controlled. The CGL system has been shown to be a clean process that does not introduce foreign contaminants. It is capable of refining tellurium as desired even with as few as three zone passes. The experiments conducted to date have shown that the system is a capable zone refiner for all of the planned studies.

REFERENCES

[1] S.M. Sze, *Modern semiconductor device physics*, New York; Chichester, England: John Wiley, 1998.

[2] F.A. Kröger, *The chemistry of imperfect crystals,* Amsterdam: North-Holland Pub. Co., 1973.

[3] A.B. Bollong and P.B. Roelof, "The ultrapurification of tellurium," *Journal of Metals,* vol. 41, pp. 39-41, July 1989. 1989.

[4] D.S. Prasad, C. Sudheer, N.R. Munirathnam and T.L. Prakash, "Tellurium purification: Various techniques and limitations," *Bulletin of Material Science,* vol. 25, pp. 545-547, 2002.

[5] W.C. Cooper, *Tellurium,* Toronto: Van Nostrand Reinhold Co., 1971.

[6] D.L. Mackay, "Pre-History of Zone-Refining," *Trends in Biochemical Science,* vol. 4, pp. N33-N33, 1979.

[7] W.G. Pfann, *Trans. AIME* 194, pp. 747, 1952.

[8] W.G. Pfann, "How Zone-Melting was Invented," *Progress in Crystal Growth and Characterization of Materials,* vol. 6, pp. R3-R4, 1983.

[9] W.G. Pfann, *Zone melting,* New York: Wiley, 1966.

[10] W.G. Pfann, C.E. Miller and J.D. Hunt, "New Zone Refining Techniques for Chemical Compounds," *The Review of Scientific Instruments,* vol. 37, pp. 649-&, 1966.

[11] C.D. Ho, H.M. Yeh and T.L. Yeh, "Simulation of multipass zone-refining processes," *International Journal of Modelling and Simulation,* vol. 23, pp. 85-93, 2003.

[12] C.D. Ho, H.M. Yeh, T.L. Yeh and H.W. Sheu, "Simulation of multipass zone-refining processes with variable distribution coefficients," *Journal of the Chinese Institute of Chemical Engineers,* vol. 29, pp. 65-71, 1998.

[13] C.D. Ho, H.M. Yeh, T.L. Yeh and H.W. Sheu, "Simulation of multipass zone-refining processes within whole ingot," *Journal of the Chinese Institute of Chemical Engineers,* vol. 28, pp. 271-279, 1997.

[14] C.D. Ho, H.M. Yeh and T.L. Yeh, "Simulation of multipass zone-refining processes," *International Journal of Modelling and Simulation,* vol. 23, pp. 85-93, 2003.

[15] G.H. Rodway and J.D. Hunt, "Optimizing zone refining," *Journal of Crystal Growth,* vol. 97, pp. 680-688, 10. 1989.

[16] J.A.J. Spim, M.J. Bernadou and A. Garcia, "Numerical modeling and optimization of zone refining," *Journal of Alloys and Compounds,* vol. 298, pp. 299-305, 2/28. 2000.

[17] C.D. Ho, H.M. Yeh and T.L. Yeh, "The optimal variation of zone lengths in multipass zone refining processes," *Separation and Purification Technology,* vol. 15, pp. 69-78, 1/4. 1999.

[18] G.S. Roussopoulos and P.A. Rubini, "A thermal analysis of the horizontal zone refining of indium antimonide," *Journal of Crystal Growth,* vol. In Press, Corrected Proof.

[19] A. Zaiour and B. Hamdoun, "Effect of temperature on segregation coefficients of impurities in tellurium," *Physica Scripta*, vol. 70, pp. 193-196, AUG-SEP. 2004.

[20] H. Schildknecht, *Zone melting,* New York: Academic Press, 1966.

[21] J.K. Kennedy and G.H. Moates, "Continuous Horizontal Zone Refining Apparatus," *The Review of Scientific Instruments,* vol. 37, pp. 1530-&, 1966.

[22] W.G. Pfann, "Zone Refining - this Simple Technique in which a Solid is Refined by Passing a Liquid Zone through it has been of Profound Value in those Technologies that Call for Materials of Extremely High Purity," *Scientific American,* vol. 217, pp. 63-&, 1967.

[23] E. Rubinstein, M.E. Glicksman, B.W. Mangum, Q.T. Fang and N.B. Singh, "Preparation of multistage zone-refined materials for thermochemical standards," *Journal of Crystal Growth,* vol. 89, pp. 101-110, 6/1. 1988.

[24] N.R. Munirathnam, D.S. Prasad, C. Sudheer, A.J. Singh and T.L. Prakash, "Preparation of high purity tellurium by zone refining," *Bulletin of Material Science,* vol. 25, pp. 79-83, 2002.

[25] AN.R. Munirathnam, D.S. Prasad, C. Sudheer and T.L. Prakash, "Purification of tellurium to 6N+ by quadruple zone refining," *Journal of Crystal Growth,* vol. 254, pp. 262-266, 6. 2003.

[26] T.F. Ciszek, "A graphical treatment of combined evaporation and segregation contributions to impurity profiles for zone-refining in vacuum," *Journal of Crystal Growth,* vol. 75, pp. 61-66, 5/1. 1986.

[27] A. Zaiour, M. Hage-Ali, J.M. Koebel and P. Siffert, "Effective and equilibrium evaporation coefficients of some impurities in molten tellurium," *Materials Science and Engineering B*, vol. 3, pp. 331-334, 8. 1989.

[28] S.R. Collins, "Stainless Steel for Semiconductor Applications," *Proceedings of the 39th Mechanical Working and Steel Processing Conference of the Iron and Steel Society*, 1998, pp. 607-619.

[29] Automation Creations Inc., "Matweb material property data," October 27, 2004. www.Matweb.com.

[30] R.G. Jordan, "Electrotransport in Solid Metal Systems," *Contemporary Physics,* vol. 15, pp. 375-400, 1974.

[31] C.A. King and S.V. Brown, "The Combination of Electrotransport and Zone-Refining Techniques for the Growth and Purification of Metallic Crystals," *The Review of Scientific Instruments,* vol. 63, pp. 3185-3187, MAY. 1992.

[32] P. Dold and K.W. Benz, "Rotating magnetic fields: fluid flow and crystal growth applications," *Progress in Crystal Growth and Characterization of Materials*, vol. 38, pp. 7-38, 1999.

[33] M.P. Volz, J.S. Walker, M. Schweizer, S.D. Cobb and F.R. Szofran, "Bridgman growth of germanium crystals in a rotating magnetic field," *Journal of Crystal Growth*, vol. 282, pp. 305-312, 9/1. 2005.

[34] S. Yesilyurt, S. Motakef, R. Grugel and K. Mazuruk, "The effect of the traveling magnetic field (TMF) on the buoyancy-induced convection in the vertical Bridgman growth of semiconductors," *Journal of Crystal Growth*, vol. 263, pp. 80-89, 3/1. 2004.

ADDITIONAL REFERENCES

V. Hoffmann, M. Kasik, P.K. Robinson and C. Venzago, "Glow discharge mass spectrometry," *Analytical and Bioanalytical Chemistry*, vol. 381, pp. 173-188, JAN. 2005.

F.L. KING, J. TENG and R.E. STEINER, "Glow-Discharge Mass-Spectrometry - Trace-Element Determinations in Solid Samples," *Journal of Mass Spectrometry*, vol. 30, pp. 1061-1075, AUG. 1995.

D.M. Chizhikov and V.P. Schastlivyi, *Tellurium and the tellurides,* Wellingborough: Collet's, 1970.

C.J. Dohrty and W.G. Pfann, "Problem of Tube Breakage in Zone-Refining, and a Solution," *Separation Science,* vol. 8, pp. 593-597, 1973.

A.D. White, "A Simple Illustration of Zone-Refining," *Journal of Chemical Education,* vol. 63, pp. 514-515, JUN. 1986.

C.K. Ghaddar, C.K. Lee, S. Motakef and D.C. Gillies, "Numerical simulation of THM growth of CdTe in presence of rotating magnetic fields (RMF)," *Journal of Crystal Growth,* vol. 205, pp. 97-111, 8/15. 1999.

O.N. Carlson and F.A. Schmidt, "Electrotransport of solutes in rare earth metals," *Journal of the Less Common Metals,* vol. 53, pp. 73-84, 5. 1977.

D. Fort, "The purification and crystal growth of rare earth metals using solid state electrotransport," *Journal of the Less Common Metals,* vol. 134, pp. 45-65, 8. 1987.

J.D. Verhoeven, "Electrotransport - as a Means of Purifying Metals," *Journal of Metals,* vol. 18, pp. 26-31, 1966.

W.G. Pfann, "Electrotransport," *Journal of Metals,* vol. 18, pp. 410, 1966.

M.M. Lopez, L. Colombo and M.J. Brau, "Electromigration of Impurities in Tellurium," *Proceedings of the Symposium on Electromigration of Metals*, pp. 35-37, Oct. 7-12, 1984.